Green Synthesis of Silver Nanoparticles using Azadirachta Indica Leaf Extract for the Application in Cotton Fibres as Antibacterial Coatings

By

Mrinmoy Mondal

MASTER OF SCIENCE IN PHYSICS

Department of Physics

BANGLADESH UNIVERSITY OF ENGINEERING AND TECHNOLOGY

November 2021

The thesis titled **"Green Synthesis of Silver Nanoparticles using Azadirachta Indica Leaf Extract for the Application in Cotton Fibres as Antibacterial Coatings"** submitted by **Mrinmoy Mondal,** Roll No.: 0417142510, Session: April 2017, has been accepted as satisfactory in partial fulfillment of the requirement for the degree of MASTER OF SCIENCE IN PHYSICS on 27 November, 2021.

BOARD OF EXAMINERS

1.	Dr. Parvin Sultana Associate Professor, Department of Physics, BUET	Chairman (Supervisor)
2.	Dr. Md. Rafi Uddin Professor & Head, Department of Physics, BUET	Member (Ex-officio)
3.	Dr. Mohammed Abdul Basith Professor, Department of Physics, BUET	Member
4.	Dr. Mohammad Abu Sayem Karal Professor, Department of Physics, BUET	Member
5.	Dr. Mohammed Nazrul Islam Khan Chief Scientific Officer, Materials Science Division Bangladesh Atomic Energy Center, Dhaka-1000	Member (External)

CANDIDATE'S DECLARATION

It is hereby declared that this thesis or any part of it has not been submitted elsewhere for the award of any degree or diploma.

Signature of the candidate

(Mrinmoy Mondal)

Roll No. 0417142510

Session: April-2017

Dedicated
To
My Beloved Parents and Teachers

Acknowledgements

Firstly, I am grateful to the Almighty, who gives me the strength, courage, patience and ability to complete this research work successfully.

Secondly, I would like to express my sincere gratitude to my supervisor Dr. Parvin Sultana, Associate Professor, Department of Physics, Bangladesh University of Engineering and Technology (BUET), Dhaka, Bangladesh, for her thoughtful guidance and constant support during my M. Sc. study and research period. Especially for her generosity, she showed up on her time despite her busy schedule. She is an excellent advisor who helped me through all the difficulties I encountered in my study, research, and life. It is my great honour to be her student. What I learned from her will benefit my whole life.

I am thankful to Prof. Dr. Md. Rafi Uddin, Head, Department of Physics, BUET, for providing me necessary facilities to carry out this research work.

I express my gratitude to Prof. Dr. Md. Abu Hashan Bhuiyan, Former Professor, Department of Physics, BUET, for his constructive criticism, encouragement, and help.

I am thankful to all other respected teachers of the Department of Physics, BUET, for their inspiration and constructive suggestions.

I sincerely acknowledge the Committee for Advanced Studies and Research (CASR), BUET, for providing me the required financial grant for this research. I am grateful to the Nanotechnology Research Laboratory and Department of Chemistry, BUET, for UV-Visible spectroscopy measurement. I sincerely thank Professor Tetsu Mieno, Shizuoka University, Japan, for the TEM measurement.

I express my heartfelt gratitude to my parents and other family members for their constant support, encouragement, sacrifices and love during this research work.

Mrinmoy Mondal

November -2021

Abstract

The present investigation reports a facile, eco-friendly, economical method for synthesizing stable silver nanoparticles (AgNPs) at room temperature using *Azadirachta indica* (neem) leaf extract as the reducing, capping and stabilizing agent. A visual colour change primarily confirmed the formation of AgNPs. The UV-visible spectroscopy analysis was performed for further confirmation and showed that surface plasmon resonance peaks varied from 425 to 436 nm depending upon the concentration of the silver salt. Structural analysis revealed that AgNPs exhibit face-centered cubic crystal structure with preferential orientation along (111) plane and the average crystallite size was ~ 20 nm. The surface morphology of the synthesized AgNPs was investigated using Field Emission Scanning Electron Microscopy and Transmission Electron Microscopy imaging, which showed that the synthesized NPs were spherical and average size varied from 27 to 32 nm. Energy Dispersive X-ray Spectroscopy analysis confirmed the presence of silver. Fourier Transform Infrared spectroscopy revealed that biomolecules present in the leaf extract acted as reducing and capping agents. The thermal stability of AgNPs was studied by TGA and DSC analyses. The zeta potential measurement showed a negative value of ~ -23.2 mV that proved the stability of AgNPs. Further, synthesized AgNPs were incorporated onto oxygen plasma-treated cotton fibres to test their antibacterial efficacy and they exhibited good antibacterial activity against *Escherichia coli* and *Staphylococcus aureus* bacteria. Hence, these antibacterial cotton fibres have great potential for utilization in burn/wound dressings and the fabrication of antibacterial textiles finishing.

.

Contents

List of Figures

List of Tables

List of Abbreviations

NPs	Nanoparticles
AgNPs	Silver Nanoparticles
DNA	Deoxyribonucleic Acid
SPR	Surface Plasmon Resonance
UV-vis	Ultraviolet-visible
FTIR	Fourier Transform Infrared Spectroscopy
FESEM	Field Emission Scanning Electron Microscopy
TEM	Transmission Electron Microscopy
EDS	Energy Dispersive Spectroscopy
EDX	Energy Dispersive X-ray
TGA	Thermogravimetric Analysis
DSC	Differential Scanning Calorimetry
DI	De-ionized
RF	Radio Frequency
FWHM	Full Width at Half Maximum
SDD	Silicon Drift Detectors
KB	Kirby-Bauer
ZoI	Zone of Inhibition
ROS	Reactive Oxygen Species
ATP	Adenosine Triphosphate

CHAPTER 1

INTRODUCTION

1.1 Background

Nanotechnology is an emerging field of research with various applications in science and technology. It is the synthesis, design, characterization and application of nanostructures by controlling size and shape in the nano regime [1]. Nanotechnology research can be conducted in several forms like nanoparticles, nanocomposites, etc. The term “nano” has been derived from the Greek word “dwarf or miniature”. Therefore, nanotechnology deals with studying the extremely small size of particles (1-100 nm), which gives strong size-dependent physical, chemical, optical, magnetic properties, etc. Researchers have recently been paying much attention to nanoparticles due to their versatile applications in biomedicine, solar energy conversion, catalysis, sensors, wastewater treatment, food and health care, cosmetics, etc. [2, 3]. The advancement in the nanoparticles (NPs) system has drawn researchers' attention allowing them to design materials by controlling their size, shape and surface morphology [4].

Metal NPs have drawn great scientific interest as they exhibit unique physicochemical properties due to their high surface-to-volume ratio. The change of energy level from continuous to discrete band with the decrease in particle size in nano regime gives strong size-dependent properties different from the same material in bulk. They exhibit enhanced catalytic activity, antibacterial efficacy, etc. [5-8]. Noble metal NPs such as silver, gold and platinum received significant attention for their remarkable antimicrobial properties [8]. Among various noble metal NPs, AgNPs are well-known biocidal substances used as antimicrobial agents in pharmacology, textiles, wound dressings, water purification systems, and medical as well as household products.

In general, there are two types of synthesis routes to fabricate AgNPs. One is the “top-down” approach, and another is the “bottom-up” approach. The top-down method is mainly the physical method of synthesizing nanoparticles by specialized ablations such as thermal decomposition, mechanical grinding, etching, cutting and sputtering of bulk material to get nano-sized particles. The main limitation of this method is the surface

structural defects that significantly impact the physical features and surface chemistry of metallic NPs. Moreover, physical methods are expensive because they require a constant energy supply to maintain high pressure and temperature. Also, the equipment is highly sophisticated [9-12]. The bottom-up approach is the preparation of material from the bottom: atom by atom, molecule by molecule or cluster by cluster. This approach includes chemical and biological processes. The chemical synthesis method can be subdivided into chemical reduction, electrochemical, irradiation-assisted chemical and pyrolysis methods [13, 14]. The synthesis of AgNPs in solution requires metal precursor, reducing agents and stabilizing or capping agents. In chemical methods, the most commonly used chemical reductants are ethylene glycol, ascorbic acid, alcohol, borohydride, sodium citrate, hydrazine compounds, etc. [15]. However, chemical processes are suitable for large-scale production but require strong reducing agents or toxic chemicals and produce harmful byproducts and thus, raising hazardous impacts on the environment and limiting their biomedical applications [16, 17]. Hence, the need for eco-friendly and non-toxic synthetic protocols for synthesizing AgNPs led to the biological approach, which is facile, biocompatible and economical.

The biological synthesis method utilizes eco-friendly resources such as plant extracts, bacteria, fungi, yeasts, etc. [18-21]. The biological techniques are well-known as ‘Green synthesis’ since they use non-toxic solvents such as water, natural extracts, and biological systems. Consequently, they are suitable for biomedical and pharmaceutical applications. One of the possible options to achieve this goal is to use microorganisms to synthesize AgNPs. Many investigations have already been done, such as synthesizing AgNPs using fungi like *Fusarium oxysporum* and *Trichoderma harzianum* [22, 23]. But synthesis using microbes is not commercially viable because it requires highly hygienic conditions for maintenance and culturing microbes is very complex as well as a slow process [24]. Plant-mediated green synthesis of AgNPs is gaining more attention among researchers than other biological approaches. It has advantages such as being facile, safe to handle, and having a faster synthesis rate as there is no need to maintain specific media and cell culture preparation process [25-29]. Natural plant extracts contain many phytochemicals such as alkaloids, flavonoids, terpenoids, phenolic compounds, proteins, etc. [30-35]. These phytochemicals are responsible for reducing metal ions to nanoparticles and can be used as capping and stabilizing agents. The use

of optimum plant extract for nanoparticle synthesis has advantages over other biological processes because it can be suitably scaled up for large-scale production.

The present study aims to apply a biological green technique to fabricate AgNPs using *Azadirachta indica* (*A. indica*) leaf extract. *A. indica*, locally known as Neem, is a common plant in our sub-continent belonging to the Meliaceae family. It is a medicinal plant and each part of this tree has been used as a household remedy against various human diseases and to treat bacterial, fungal, viral, and many skin ailments. Phytochemicals like flavanones and terpenoids are abundant in the leaf extract of *A. indica* and play a vital role in synthesizing AgNPs. They act as both reducing and capping agents [36, 37]. Roy *et al*. [36] reported the green synthesis of AgNPs using *A. indica* leaf extract. They varied the leaf extract concentration and showed surface plasmon resonance (SPR) peaks in the 420-450 nm range. They reported that their prepared nanoparticles had a wide size distribution and showed antibacterial activity against both Gram-negative and Gram-positive bacteria. However, structural and surface morphological properties were not examined, despite the fact that they are crucial for determining the average size and shape of the prepared sample. Because the SPR peak depends on the size and shape of the nanoparticles. Since prepared nanoparticles have a tendency to agglomerate and form larger-sized particles, it is vital to know the dispersion stability of the sample. Further information about chemical bonding is crucial to identify which phytochemicals are responsible for redox reactions and stabilization. Therefore, there is much scope to synthesize the sample by varying the salt concentration, pH of the solution and reaction time and study the characterization mentioned above to gain in-depth knowledge about the sample. Furthermore, they didn’t prepare any composite material using their prepared AgNPs that can be utilized in various biomedical and medical sectors. So, we intended to biologically synthesize AgNPs and combine them with cotton fibres to prepare AgNP/cotton composite fibres for practical use in different biomedical and medical fields.

The demand for the fabrication of antibacterial textiles using the green synthesis route has been rapidly growing over the last few decades [38]. The reason is for their promising applications in medical, health care and hygienic products, protective textile materials, etc. [39, 40]. Cotton fibres are particularly suitable for manufacturing textiles for sports, non-implantable medical products, and sterile products [41]. However, cotton can absorb a significant amount of moisture and act as a medium for microorganism

growth as pathogenic or odor-generating bacteria and fungi under specific temperature and humidity conditions [42, 43]. In contact with the human body, these microorganisms get an ideal environment for growth, having a large surface area and retaining oxygen and moisture. Therefore, the antibacterial coatings on the surface of cotton can be applied to get better antimicrobial cotton textiles. AgNPs exhibit strong antibacterial effects among various antimicrobial agents and can prevent or minimize infection with pathogenic bacteria. This fabrication process can be carried out using chemical and biological routes. Pad dry cure method is widely used to incorporate AgNPs onto cotton fabrics [44, 45]. It is a multi-step process and requires a high-pressurized instrument for padding AgNPs. It is also important to maintain a fixed curing temperature; if not, the fabric can be deformed. The green synthesis route can solve these problems because it can be performed at room temperature and this one-step process does not require curing cotton fibers [46]. Since environmentally benign materials and energy efficient synthesis route is used to prepare AgNPs, it may address the growing concern about environmental exigency.

The incorporation of AgNPs onto the cotton fibres largely depends on the surface structure of cotton fibres. Cotton fibres having hydrophilic properties and less hemicellulose can absorb more AgNPs. So it is also important to functionalize cotton fibres by a surface modification to get better results. Alkali and low-temperature oxygen plasma treatment are commonly used for surface modifications [47]. These treatments reduce cellulosic compounds and make cotton fibres more hydrophilic.

The purpose of this study is two-fold. Firstly, the synthesis of greener AgNPs using *A. indica* leaf extracts and the fabrication of AgNPs coated cotton fibres for their practical application as antibacterial cotton fibres. To the best of our knowledge, there is no report on the fabrication of AgNPs coated antibacterial cotton fibres using *A. indica* leaf extract.

1.2 Objectives of the Present Study

The objectives with specific aims are as follows:

i. Synthesis of AgNPs and AgNPs incorporated cotton fibres via a green approach using *A. indica* leaf extracts.

ii. Study the optical properties and dispersion stability using UV-vis spectroscopy and Zeta potential measurement.
iii. Investigation of the crystalline structure and functional groups of AgNPs using X-ray diffraction (XRD) pattern and Fourier Transform Infrared (FTIR) spectroscopy.
iv. Study the surface morphology of synthesized samples through Field Emission Scanning Microscopy (FESEM) and Transmission Electron Microscopy (TEM).
v. Study the thermal stability of both AgNPs and AgNPs loaded cotton fibres by Thermogravimetric Analysis (TGA) and Differential Scanning Calorimetry (DSC).
vi. Investigation of the antimicrobial efficacy of AgNPs and AgNPs coated cotton fibres against Gram-positive and Gram-negative bacteria using the agar well diffusion method.

1.3 Outline of the Thesis

The main purpose of the research work is to synthesize AgNPs via the green synthesis route and to fabricate AgNPs coated antibacterial cotton fibres. The thesis has been organized as follows:

Chapter 1 of this thesis discussed the introduction and importance of the green synthesis of AgNPs along with specific aims and objectives.

Chapter 2 described the literature review of the present state of AgNPs synthesis.

Chapter 3 discussed the sample preparation technique and different characterization techniques required for analyzing green synthesized AgNPs and AgNPs coated cotton fibres.

Chapter 4 presented experimental results and possible discussions based on the results.

Chapter 5 described the present work's summary and concluding remarks and scope for future work.

CHAPTER 2

LITERATURE REVIEW AND THEORETICAL ASPECTS

2.1 Previous Reports on the Synthesis of AgNPs

Many research works have been done on the synthesis of AgNPs. When bulk silver is reduced to nanosilver, it exhibits remarkable changes in its different properties, making it more valuable from the application point of view. Since then, many researchers have synthesized AgNPs using different methods. Some researchers utilized the green synthesis technique to synthesize AgNPs. A few of them synthesized AgNPs to incorporate them onto cotton fibres to investigate antibacterial activity against some bacteria. Some of the works are discussed below.

M. C. Lea synthesized the first nanosilver or AgNPs in 1889. He used citrate to stabilize AgNPs and the average size was between 7 to 9 nm [48].

The Pulsed laser ablation method is one of the most popular techniques for synthesizing AgNPs. Zamiri *et al.* [12] prepared AgNPs in natural polymers assisted by the pulsed laser ablation method. An Ag plate (99.99% purity) was irradiated by a Q-switched Nd: YAG pulsed laser of wavelength 532 nm and energy 360 mJ/pulse. Silver atoms were ejected from the metal surface by the local high temperature and plasma plumes of high pressure. Then the ejected silver ions formed AgNPs through cooling and condensation. Different polymers such as gelatin, starch, and chitosan were used as stabilizers. It is a rapid and simple one-step process of preparation of AgNPs and provides a significant result. They found minimum-sized NPs using gelatin as a stabilizer. Nevertheless, the experimental setup is quite sophisticated and expensive. Moreover, it requires an external stabilizer to cap the ejected AgNPs and synthesized NPs may get agglomerated due to poor focusing conditions.

AgNPs have to be stable, small in size and narrow in size distribution for biomedical applications. The chemical reduction method is very often used to synthesize such AgNPs. Various surfactants are used to prepare controlled-size AgNPs. The main difficulty in this process is the purification of colloids from surfactants, which is important for biological applications. Wang *et al.* [13] reported the chemical synthesis of AgNPs using $AgNO_3$, glucose, polyvinyl pyrrolidone (PVP) and sodium hydroxide.

They synthesized AgNPs by reducing $AgNO_3$ in PVP, glucose and NaOH aqueous solution. The synthesized AgNPs were well dispersed with sizes ranging from 20 to 80 nm, suggesting a wide size distribution. It is crucial to maintain a suitable amount of dispersant which controls the formation and agglomeration of AgNPs. If there is a lack of dispersant, the protection layer cannot be formed, leading to aggregation. However, this is a multi-step and costly process and requires many chemical reagents. Some of them are toxic chemicals and hazardous to our environment. Sometimes bi-products come out from different reactions, which are of no use except for polluting the surroundings. So this problem led researchers to prefer the biological route to develop an eco-friendly, cost-effective and one-step process.

In the biological route, various species of fungus are widely exploited for the biogenic synthesis of AgNPs. Dameron *et al.* first utilized *Candida albicans* fungus to synthesize CdSe NPs in 1989. Guilger-Casagrande *et al.* [23] synthesized AgNPs employing *Trichoderma harzianum* fungus. At room temperature, they cultivated T. harzianum using wettable powder in potato dextrose agar medium. This fungus culture was done in the absence of light and the temperature was maintained nearly constant. Their report confirmed that the mean diameter of biosynthesized AgNPs was 57.02+/-1.75 nm and the zeta potential value was -18.70+/-3.01 mV. Biological synthesis using fungi is very lengthy process. It takes 12 to 15 days to cultivate fungi and requires extra carbon and nitrogen for growth. Then additional three days are needed to prepare fungus as a reducing agent. The reduction rate is slow and the particle size obtained was larger than plant-mediated synthesis.

Kajani *et al*. [26] synthesized anisotropic AgNPs using *Taxus baccata* extract and investigated their potent anticancer activity. They performed several characterizations to study the physical, chemical, thermal and cytotoxic properties of synthesized anisotropic AgNPs. From particle size distribution, the average size of anisotropic AgNPs was found to be ~ 91 nm. The zeta potential value was measured as -7.7 mV for optimal conditions. The thermal stability of synthesized anisotropic AgNPs was studied from TGA analysis. A weight loss of 27% was noticed at the temperature of 521 ºC and the total weight loss was about 36.89% at 700 ºC. The flower extract could be a good reducing agent, along with different plant parts. Arokiyaraj *et al*. [27] reported the synthesis of AgNPs using *Chrysanthemum indicum (C. indicum)* floral extract and studied its antibacterial and cytotoxic effects.

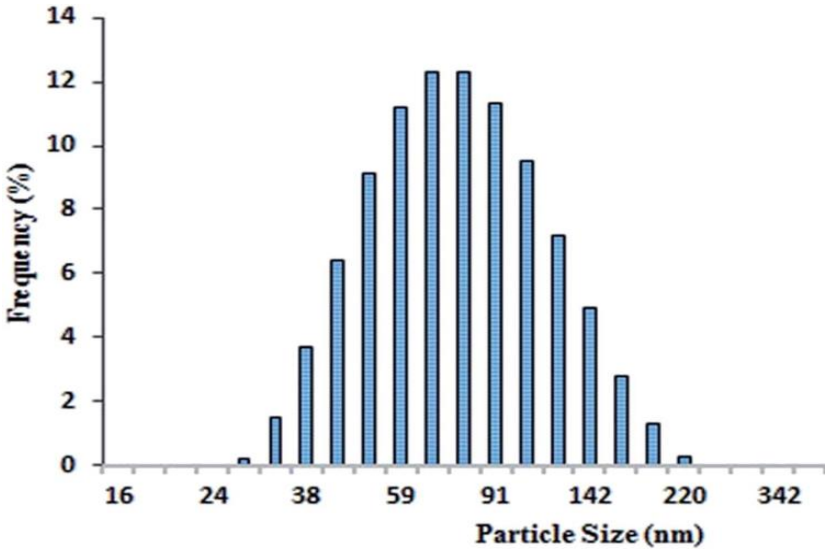

Fig. 2.1 Size distribution of anisotropic AgNPs using *Taxus baccata* extract [26].

They also characterized the optical and morphological properties of synthesized AgNPs. Their TEM micrograph revealed that the average size of AgNPs ranged from 37 nm to 71 nm. EDS analysis confirmed the presence AgNPs as the majority of the constituents. Their study confirmed that AgNPs were crystalline and exhibited face-centered cubic structure. XRD analysis showed characteristic peaks at 38º, 44º, 64º, 77º and 81º, corresponding to 111, 200, 220, 311 and 222 planes. The crystallite size calculated from the XRD pattern using Scherrer's equation was ~53 nm. This size range suggested that synthesized AgNPs had a wide size distribution.

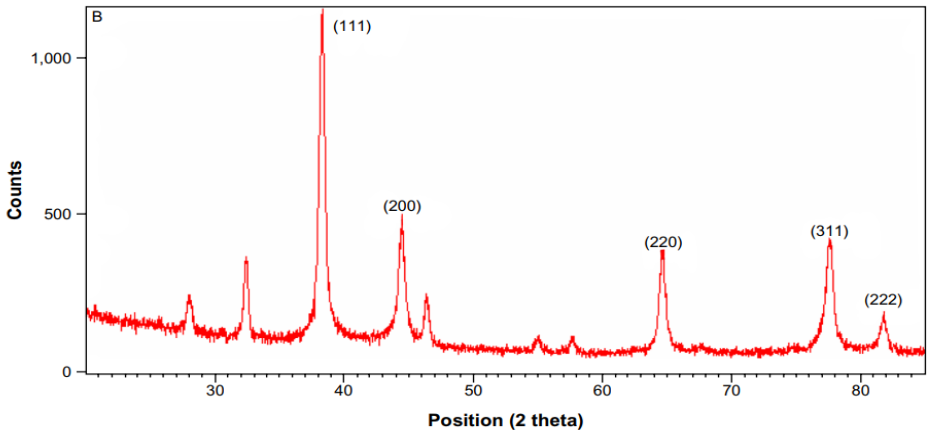

Fig. 2.2 XRD pattern of synthesized AgNPs using *C. indicum* floral extract [27].

They tested antibacterial efficacy against both gram-positive and gram-negative bacteria. Their result showed a zone of inhibition (ZoI) of 8.33+/-0.57 mm against *Staphylococcus aureus (S. aureus)* and 13+/-0.90 mm against *Escherichia coli (E. coli)* bacteria. This better efficacy against gram-negative bacteria was due to the thickness peptidoglycan layer.

Many researchers synthesized NPs using plants grown under in vitro conditions. Pirtarighat *et al.* [28] synthesized AgNPs using the green route, where they used plant extract of *Salvia spinosa* in vitro. First, the seeds of *S. spinosa* were sterilized with 70% ethanol followed by 2.5% sodium hypochlorite. Petri dishes were prepared using mineral salt, 4.5% agar and the pH was kept at 5.8. Then seeds were explanted for germination. Synthesized AgNPs were characterized with FESEM, FTIR and XRD analysis. The synthesized AgNPs exhibited good efficacy against Gram-positive and Gram-negative bacteria. But harvesting *S. spinosa* in vitro is a sophisticated and lengthy process. It requires about two months, according to their report.

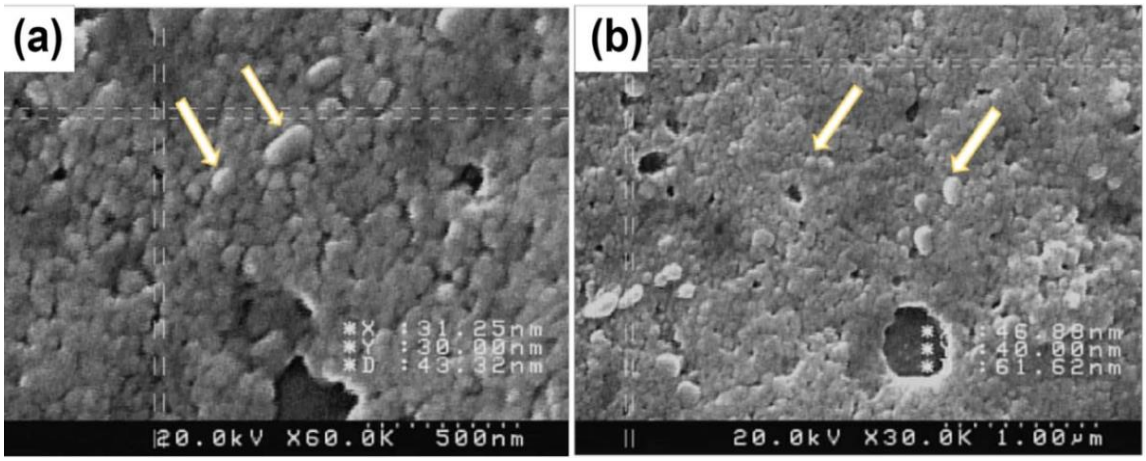

Fig. 2.3 FESEM images of biosynthesized AgNPs using *Salvia spinosa* extract [28].

The XRD pattern of their synthesized AgNPs confirmed crystalline structure, but there were few undefined peaks with high intensity. It may be due to impurities which can be a barrier to the proper use of AgNPs.

The surface morphology of synthesized AgNPs shows agglomeration. The average particle size was calculated from the FESEM image and DLS analysis. The average particle size was 19 to 125 nm in diameter according to FESEM and from DLS analysis, it was 5.13 nm. These measurements were inconsistent with each other. Moreover, synthesized AgNPs had a wide range of size distributions.

Roy *et al*. [36] reported the synthesis of AgNPs using *A. indica* and investigated their antimicrobial activity. Their study suggested that the absorbance of the synthesized AgNPs increased with the increase of leaf extract ratio with respect to $AgNO_3$. The average particle size obtained from DLS analysis was 65-67 nm in diameter and the polydispersity index varied from 0.280 to 0.299. DLS analysis revealed a wide particle size distribution. They tested their synthesized AgNPs against both gram-positive and gram-negative bacteria. They applied 20, 50 and 100 µL of synthesized AgNPs solution into the diffusion well. The ZoI varied from 8.66 mm to 22 mm depending on the amount of AgNPs solution used in a diffusion well and the condition under which the AgNPs were synthesized. They got a better antibacterial response against gram-negative bacteria and results varied from 11.83 to 16.67 mm.

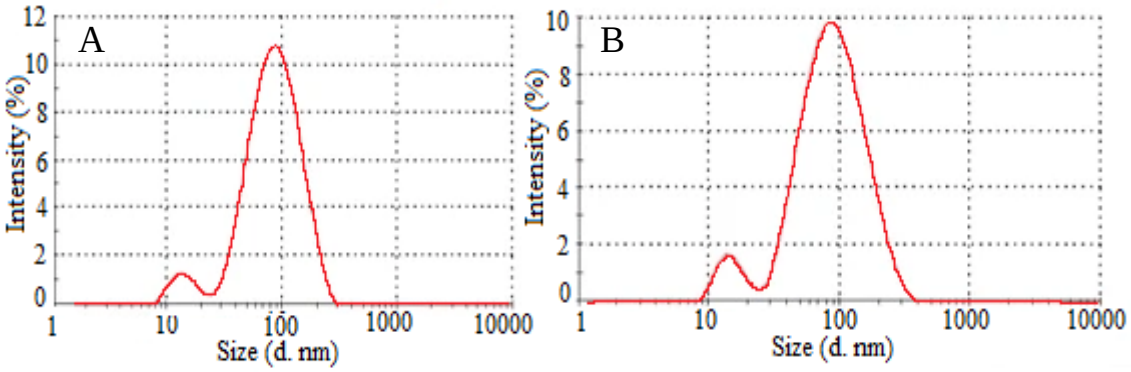

Fig. 2.4 DLS analysis of biosynthesized AgNPs using $AgNO_3$ and *A. indica* at a ratio (A) 10:1 and (B) 10:3 [36].

2.2 Previous Investigations on the Antibacterial Performance of AgNPs and AgNPs Coated Cotton Fibres

Although, in recent years many research groups have synthesized AgNPs to find potential applications in antibacterial response, photocatalytic performance, etc. The reported investigation is rare, particularly as antibacterial cotton fibres using leaf extract.

Wu *et al.* [44] fabricated antibacterial cotton fabric finishing by AgNPs using a chemical method. They synthesized AgNPs by reducing $AgNO_3$ with $NaBH_4$ in an aqueous phase. In that process, $Na_3C_6H_5O_7.2H_2O$ was used as a reducing agent and $NaBH_4$ to maintain the pH of the solution. They controlled the size of the AgNPs, adding an appropriate amount of $NH_3.H_2O$ (1.45 mol/L) and pH. Before the incorporation of AgNPs, cotton fabrics were treated with NaOH (4 g/L), citric acid (CA) (60 g/L) and $NaH_2PO_2.H_2O$ (70 g/L) at 60^oC for 30 minutes to gain a carboxyl modified surface. The incorporation of AgNPs was carried out by the pad-dry-cure method. The surface-modified cotton fabrics were then immersed into the AgNPs solution of 25 mg/L concentration and stirred for 1 hour. The AgNPs incorporated cotton fabrics were dried at 80 ℃ for 30 minutes. Finally, the samples were cured at 140 ℃ for 2 minutes.

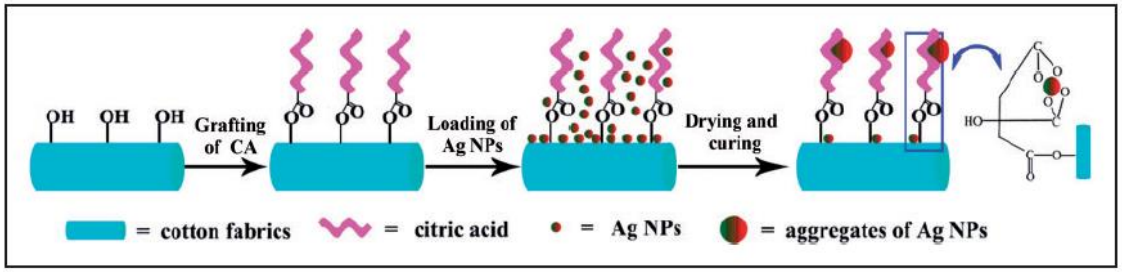

Fig. 2.5 Schematic representation of the mechanism of incorporation of AgNPs on citric acid-treated cotton fibres [44].

Fig. 2.5 shows the possible mechanism of AgNPs incorporation onto the fabrics. Carboxyl groups originated from citric acid reacted with hydroxyl that comes from cellulose. Citric acid was coated on the fabric's surface by the esterification reaction. The AgNPs were impregnated onto the fabrics through the chelation of silver and oxygen atoms. Here citric acid linked up a bridge between AgNPs and cotton fabrics.

Fig. 2.6 shows the surface morphology of the pure cotton fabrics, AgNPs incorporated cotton fabrics before and after 50 cycles of washing. Their fabricated antibacterial cotton fabrics exhibited good antibacterial activity against both gram-positive and gram-negative bacteria. This process is feasible but multi-step and requires many chemical agents. Several by-products may be produced during the synthesis of AgNPs. Moreover, during the curing process, the heat treatment of AgNPs incorporated in cotton fabrics may cause the deformation of cotton fibres.

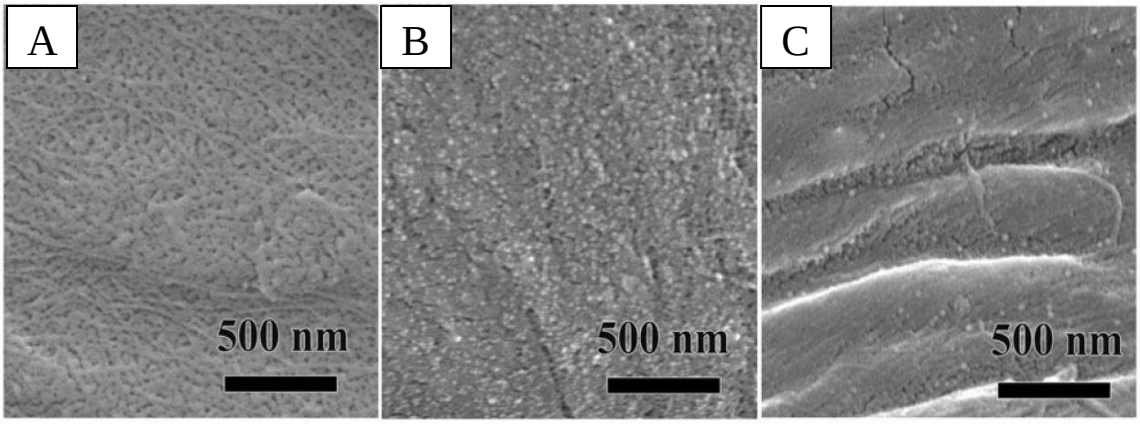

Fig. 2.6 FESEM images of cotton fabric (A) original (B) Ag-CA treated before washing (C) Ag-CA treated after washing [44].

El-Rafie *et al.* [45] biologically synthesized AgNPs, applied them to cotton fabrics, and investigated the bactericidal efficacy of the treated fabrics. They inoculated *F. solani* fungus as the source of reducing agents. They varied biomass and $AgNO_3$ concentration and pH of the solution. They observed a significant change in the reduction of Ag^+ with the increasing of pH level of the solution. The intensity of the absorbance peak increased and shifted towards the higher wavelength with the increase of pH of the medium up to 8. But the synthesized AgNPs attained better stability in the pH range of 10-12 with the blue shift of SPR peak. After synthesizing, they incorporated AgNPs onto cotton fabrics by padding method at constant pressure using a laboratory padder.

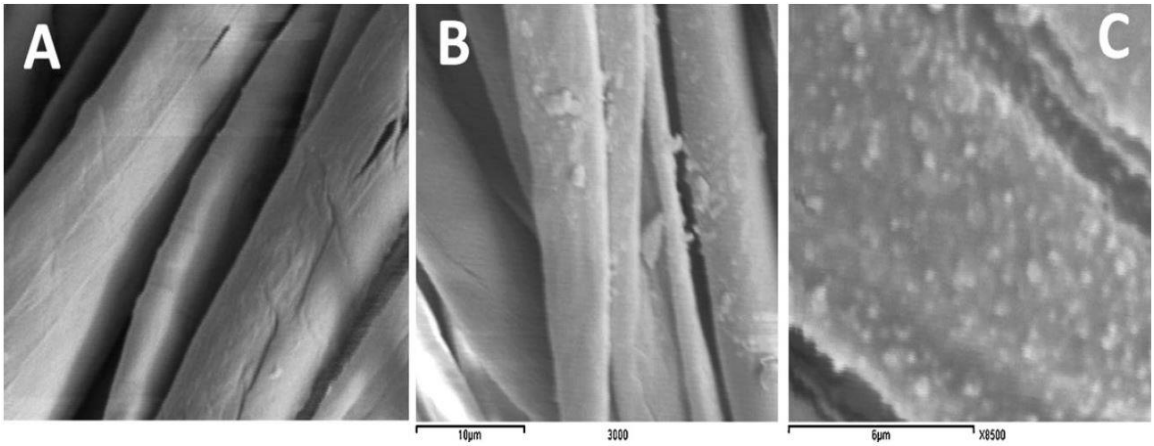

Fig. 2.7 FESEM images of cotton fabric (A) untreated, (B) and (C) AgNPs incorporated [45].

This method also needs the curing of cotton fabric after coated with AgNPs. Their study showed that the deposited amount of AgNPs onto cotton fabric was more significant at a higher concentration of AgNPs colloidal solution.

Rao *et al.* [29] reported the synthesis of AgNPs using *Eriobotrya japonica* leaf extract and investigated antibacterial activity. They performed optical, morphological, structural and elemental characterizations. The synthesized AgNPs were spherical, with a narrow size distribution ranging from 46 nm to 70 nm. They also studied the effect of reaction temperature on particle size. The average particle size was 76.1 nm synthesized at 25 ℃, whereas AgNPs synthesized at 80 ℃ had an average size of 54.47 nm in diameter. The zeta potential value of -20.4 mV indicated moderate dispersion stability. They tested the antibacterial efficiency of biosynthesized AgNPs against *E. coli* and *S. aureus* bacterial strains. Their result showed that ZoI was increased when the concentration of AgNPs increased. The maximum ZoI was about 4.5 mm for 100 mg/L concentration of AgNPs against *S. aureus* bacterium. This antibacterial efficacy is lower compared with some other reports.

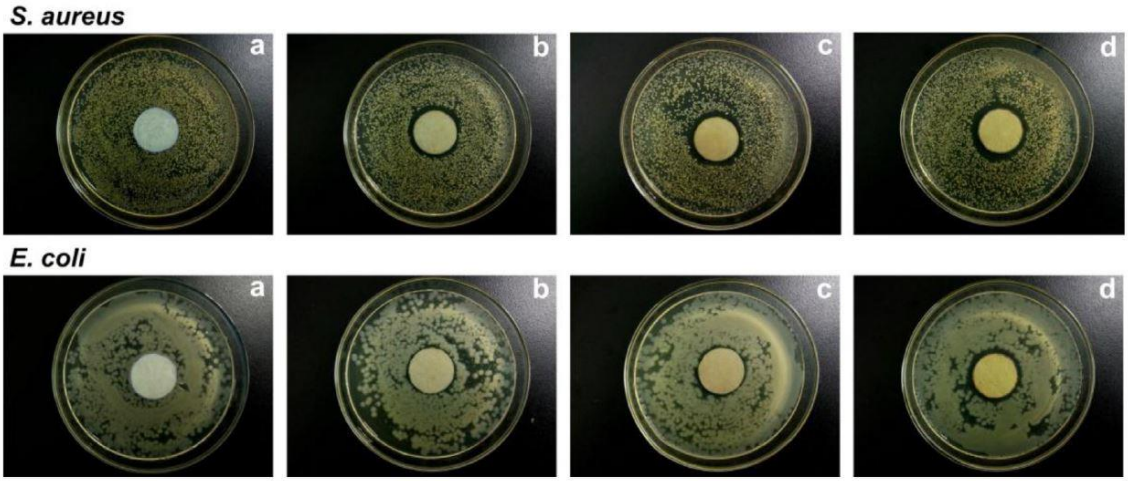

Fig. 2.8 Antibacterial activity of AgNPs against *S. aureus* and *E. coli* bacteria [29].

Ravindra *et al*. [46] fabricated antibacterial cotton fibres loaded with AgNPs via facile green synthesis using Neelagiri and Marri leaves. They investigated the antibacterial efficiency of AgNPs incorporated in cotton fibres along with its morphology, thermal and mechanical stabilities. The surface morphology of AgNPs loaded cotton fibres confirmed the deposition AgNPs onto the cotton fibres. Their analysis revealed that the incorporation of AgNPs onto the cotton fibres was enhanced with a higher leaf extract concentration. However, the structural and elemental analysis should be performed to confirm the presence of any impurities which can affect the biomedical application.

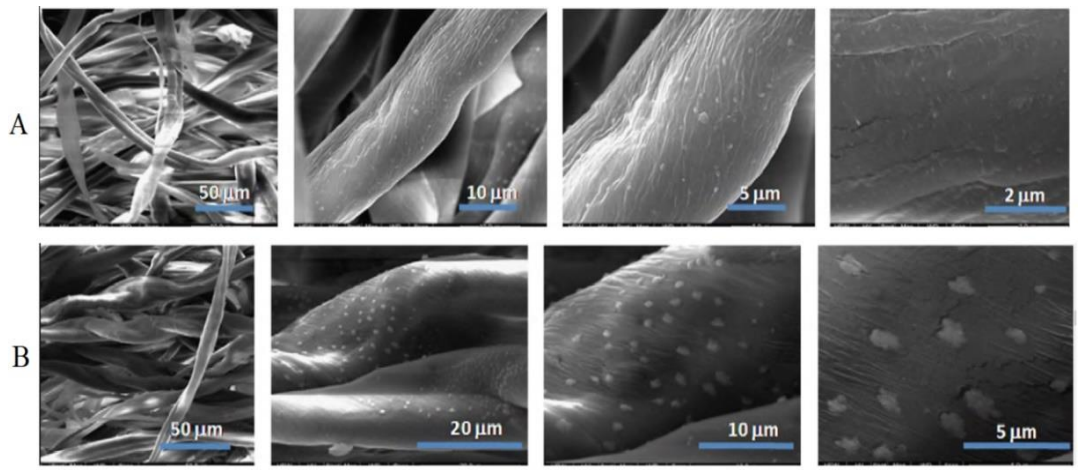

Fig. 2.9 SEM micrograph of AgNPs incorporated cotton fibres using (A) Neelagiri and (B) Marri leaves [46].

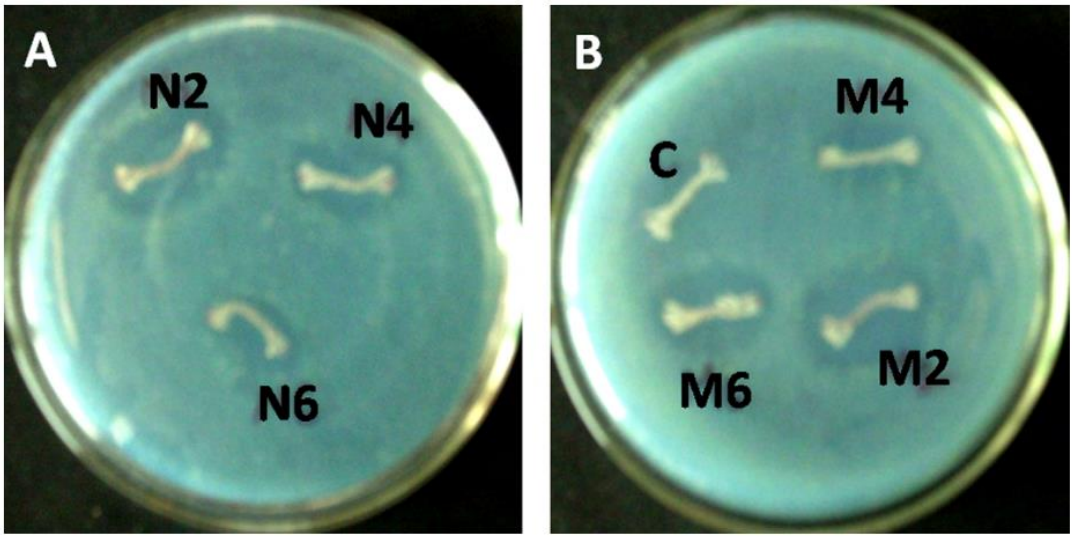

Fig. 2.10 Antibacterial activity of AgNPs loaded cotton fibres using (A) Neelagiri leaves and (B) Marri leaves [46].

Fig. 2.10 shows the antibacterial efficiency of AgNPs incorporated in cotton fibres which exhibited significant antimicrobial activity against *E. coli* bacterium. The AgNPs loaded cotton fibres should also be tested against some gram-positive bacteria, which can broaden their application in bioscience.

To the best of our knowledge, for the first time, in this investigation, the antibacterial performance of AgNPs coated oxygen plasma treated cotton fibres was carried out using *A. indica* leaf extract.

2.3 AgNPs

Silver is a soft incandescent element. Metallic silver is not soluble in water, while silver salts like silver nitrate ($AgNO_3$) and silver chloride (AgCl) are water-soluble. Nanosilver exhibits unique properties such as chemical stability, excellent electrical conductivity, catalytic activity, antibacterial efficacy, non-linear optical properties etc. [49, 50]. AgNPs are used to develop new technologies in electronics, materials science and medicine. Nanosilver is used as an antimicrobial agent in medical, environmental fields and nanoscience research.

2.3.1 Applications of AgNPs

AgNPs can be used for advanced technologies in electronics, material sciences, and medicine. Due to their comprehensive applications in different areas, more research is being conducted on the fabrication of AgNPs by researchers worldwide. Nanosilver is extensively used as an antimicrobial agent in the medical and environmental fields. Fig. 2.11 represents different applications of AgNPs.

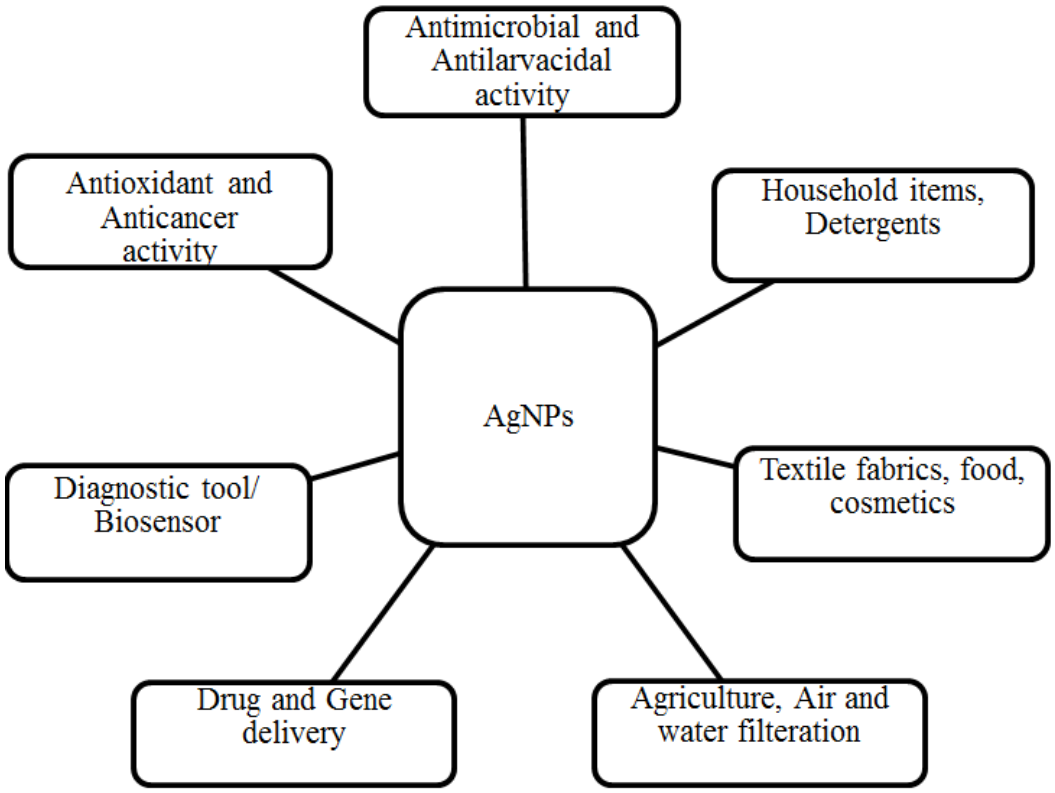

Fig. 2.11 Schematic representation of applications of AgNPs.

2.3.2 AgNPs as coating material

The green synthesized AgNPs can be incorporated into different natural fibres to provide antibacterial coatings on the surfaces of various objects such as medical products and garments [51]. These nanocoated fibres have great potential for utilization in pharmaceutical, health care, hygienic products and protective textiles. Cotton fibres are especially compatible for producing antibacterial finishing fabrics among various natural fibers.

CHAPTER 3

MATERIALS AND METHOD

In this chapter, the essential steps for synthesizing AgNPs using plant-mediated green synthesis are presented initially. Later on, the characterization techniques to investigate the optical, structural, morphological, thermal and antibacterial properties of AgNPs have been discussed.

3.1 Materials

Fresh leaves of *A. indica* (Neem) were collected from the tree which is available in the University campus. Silver Nitrate ($AgNO_3$) was purchased from Merck, India. Cotton fibres were brought from the local textile mill. Nutrient Agar plate was used to culture both gram-positive and gram-negative bacteria. For the present study, *S. aureus* and *E. coli* were cultured and used. De-ionized (DI) water was used throughout the whole research work.

3.2 Sample Preparation

3.2.1 Preparation of leaf extract

Collected leaves were washed several times in running tap water to remove dirt, dust and other contaminated organic chemicals from the surface of the leaves. Then the leaves were finally washed with de-ionized water and dried at room temperature to remove the residual moisture. The clean leaves were then cut into small pieces. All the glassware was washed with de-ionized water in an ultrasonic bath and dried in the oven. Then 20 grams of chopped leaves and 100 ml of DI water were taken in a 500 ml glass beaker and boiled for 20 minutes at 90 ℃. The leaf extract appears to be a light green colour. It was cooled down to room temperature and filtered through Whatman no.1 filter paper and stored at 4 ℃ for further use. This extract was used for the reduction of silver ions to AgNPs.

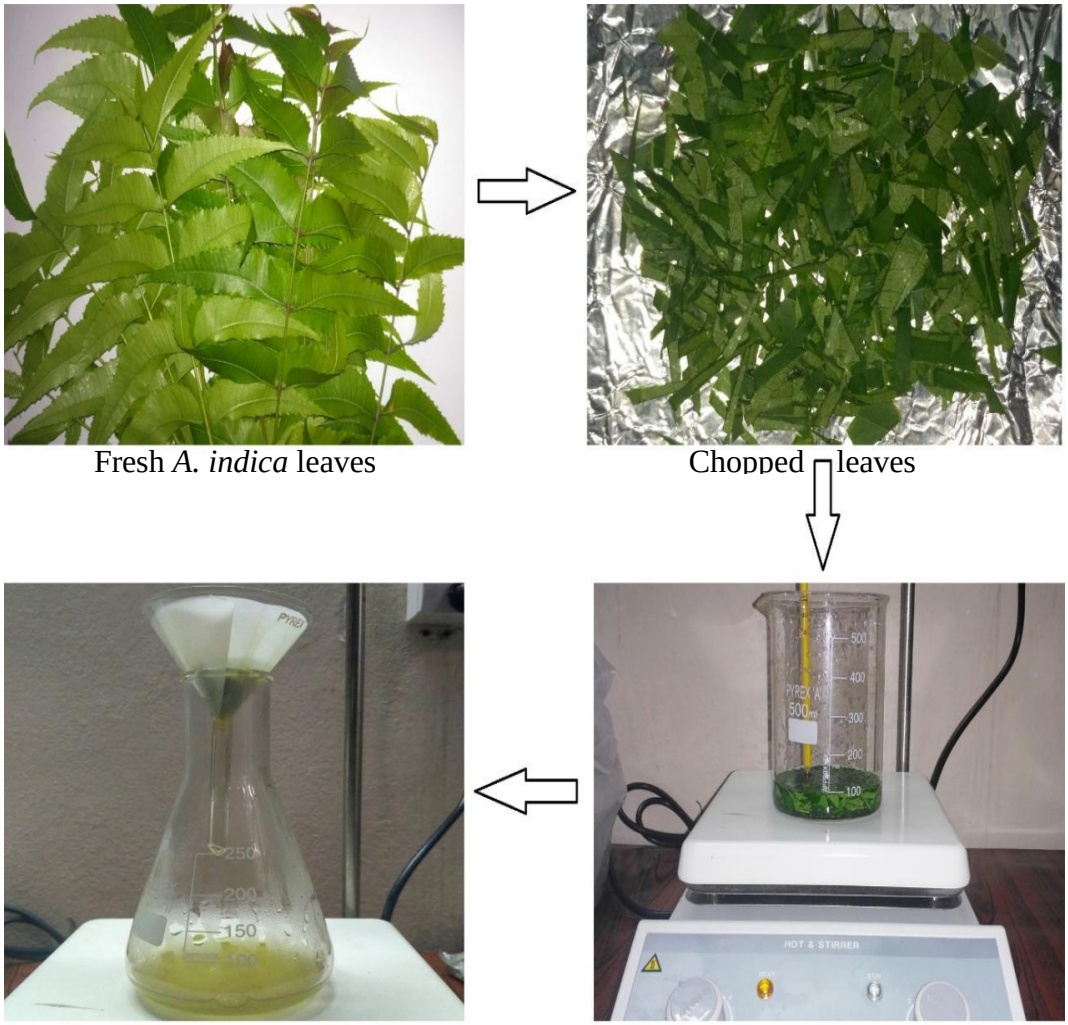

Fig. 3.1 Preparation of *A. indica* leaf extract.

3.2.2 Preparation of silver nitrate solutions

$AgNO_3$ received from Sigma Aldrich was used without further purification. 0.085 gram of $AgNO_3$ was weighed and dissolved in a 250 ml Erlenmeyer flask containing 100 ml of DI water to make 5mM of $AgNO_3$ solution. Appropriate amounts of DI water were added to the $AgNO_3$ solution to decrease the molarity to 1mM, 2 mM, 3 mM and 4 mM.

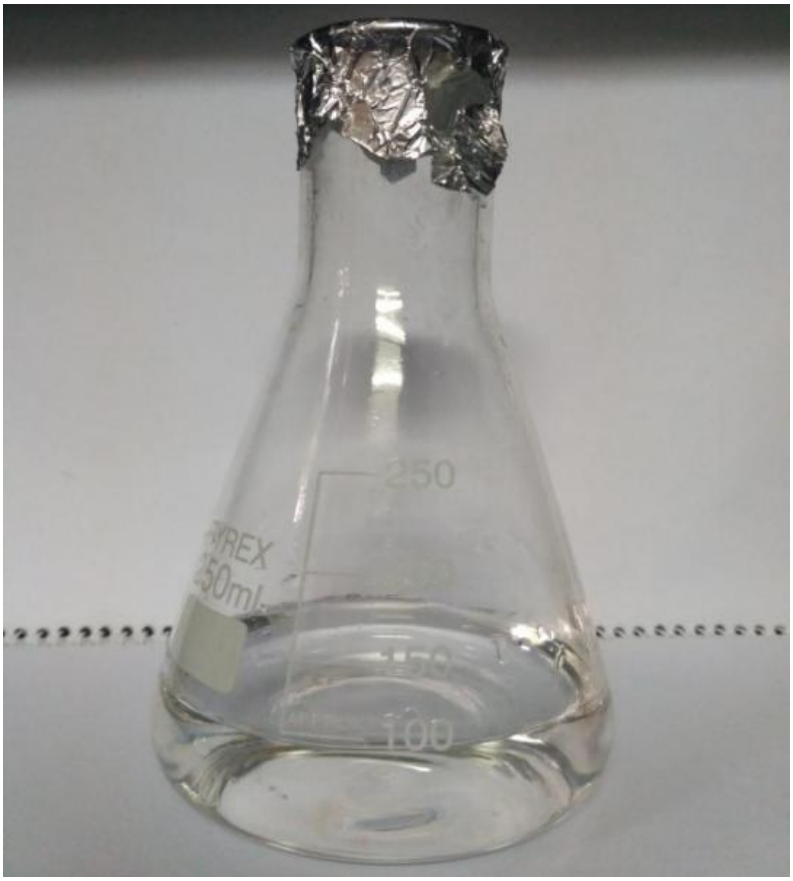

Fig. 3.2 Silver nitrate ($AgNO_3$) solution.

3.2.3 Synthesis of AgNPs

10 ml stock solutions of different concentrations (1 mM to 5 mM) of $AgNO_3$ were taken in Erlenmeyer flasks. Prepared leaf extract of 1 ml was added to each flask. The mixtures were kept in room temperature to react. Silver ions were reduced to AgNPs due to the reducing agents present in the leaf extract. The rapid conversion from Ag+ to AgNPs was observed by colour change to brown colour. Further, the leaf extract of different amounts was added to 5 mM $AgNO_3$ solution to investigate the effect of leaf extract concentration. The reduction of Ag+ and the formation of AgNPs were monitored with the help of a UV-visible spectrometer.

The following figure shows the synthesis process of AgNPs using leaf extract. The leaf extract and 1mM $AgNO_3$ solution was taken at a 10:5 ratio.

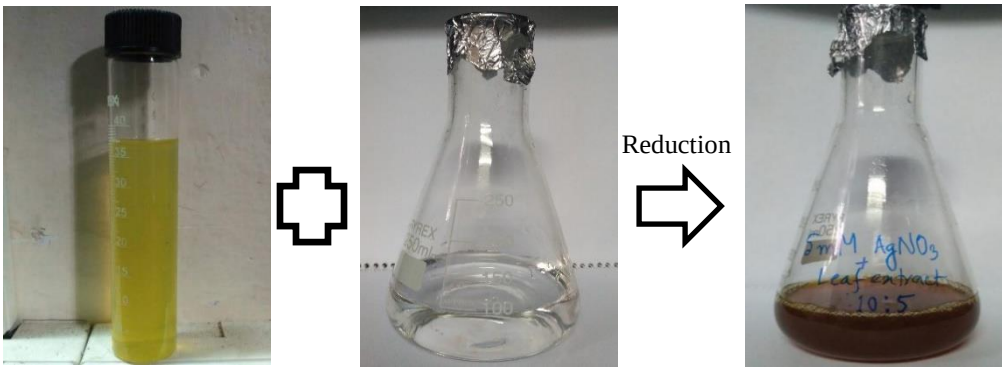

Fig. 3.3 Synthesis of AgNPs using *A. indica* leaf extract.

The solution containing AgNPs of different concentrations was centrifuged using a centrifuge machine (DLAB-0412, USA) at 4500 rpm for 20 minutes. Then the precipitate was collected and dried in a hot air oven at 90 ℃ for 3 hours. The dried AgNPs powder was ground using a hand mortar and characterized using various analytical instruments.

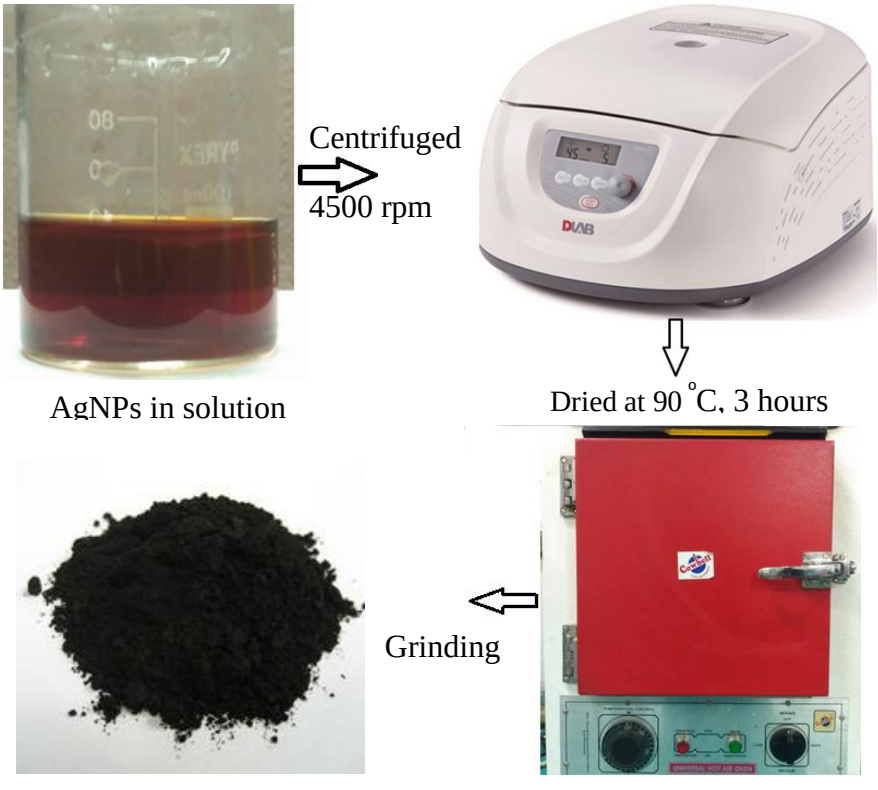

Fig. 3.4 Process of preparing AgNPs powder from solution.

3.2.4 Cotton fibres

Cotton is a natural cellulose fibre and is used in textiles worldwide. It comprises cellulose and some non-cellulosic modules such as proteins, waxes, pectic substances, organic sugars and acids [52]. It has hydroxyl groups on the surface. It is inherently inconsistent with hydrophobic polymer matrix materials and exhibits poor interfacial adhesion between the hydrophilic natural fibres and matrix materials [53]. Textiles from natural fibres such as cotton are more susceptible to microbe attack due to their higher moisture absorption ability. Therefore, cotton fibres need to be processed to functionalize and achieve antimicrobial properties. Antimicrobial finishing can protect textiles from microbial attack, enhance durability and protect the wearer from microbial infections. Due to the ongoing pandemic, antimicrobial coating on textiles is becoming a highly important issue and has gained significant attention. Cotton fibres were firstly Alkali treated, then washed in an acidic medium, and finally treated with oxygen plasma.

3.2.5 Treatment of cotton fibres

The untreated cotton fibres were passed through alkali and oxygen plasma treatment. Alkali treatment of cotton fibres also removed cellulose, proteins, and other organic acids. Then surface modification of alkali-treated cotton fibres was executed using a plasma system with RF oscillator. The whole process of treatment was performed in the following steps.

3.2.6 Alkali treatment of cotton fibres

Alkali treatment of cotton fibre removes most of the cellulose, organic acids and pectins from the surface of the cotton fibres. This process gives cotton fibres a high tensile strength and makes the fibres useful for the production of reinforced composites. Moreover, alkali treatment increases mechanical properties and the cotton fibres turn into hydrophobic from hydrophilic through this process. After alkali treatment, cotton fibres should be washed with an acidic medium to remove the residual alkaline substances.

1 gm of control cotton fibre was taken and washed with running water followed by DI water to remove dirt from the surface. 5% of NaOH solution of 30 ml was prepared taking 0.05 gm of NaOH and dissolving into 30 ml of DI water. Cotton fibres were

deeply washed by NaOH solution for 1 hour, followed by DI water. Alkali treated cotton fibres were then dried to remove water and moisture.

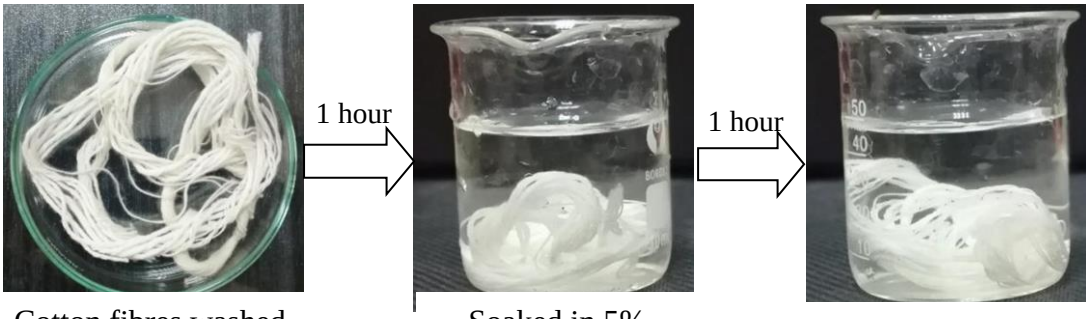

Fig. 3.5 Alkali treatment process of cotton fibres.

However, some residual NaOH might remain with cotton fibres after washing with DI water. Dried cotton fibres were further treated with Acetic acid solution to neutralize the excess alkali. The acidic acid solution was prepared by taking 15% pure acetic acid. After washing for 1 hour, the cotton fibres were rinsed with DI water. The treated cotton fibres were then dried and prepared for plasma treatment.

3.2.7 Plasma treatment of cotton fibres

Low-temperature plasma treatment process is widely used in textile areas to modify the surfaces of natural fibres like cotton. It improves dyeability, printability, wettability, water and oil-repellent, and antimicrobial properties [54-57]. Free electrons of plasma attain energy from the radio-frequency electric field and form reactive species by colliding with neutral gas and transferring energy dissociating the molecules. The interaction of these excited species chemically and physically modifies the material surface. Plasma treatment plays a dual role for the cotton fibres: it functionalizes the surface of the cellulose substrate and plasma may act as a medium for the final deposition of antimicrobial agents [58].

Low-pressure oxygen plasma affects surface morphology and enables chemical modification of cotton fibres by introducing new functional groups and active species that alter the reactivity of the substrate [59].

The low-pressure plasma system comprised an RF generator (ENI, ACG-6B) of frequency 13.56 MHz, a pair of copper electrodes, each having a diameter of 8 cm and a thickness of 1 mm. A rotary pump, Pirani gauge and an airtight cylindrical glass chamber of diameter 6 inches and length 8 inches were connected with an oxygen cylinder. The glass chamber was cleaned with DI water and acetone. Then, alkali-treated cotton fibres were kept in a petri dish on the fixed electrode inside it. The rotary pump was kept on until pressure inside the chamber became 0.5 torrs. Then the RF generator was turned on and a frequency of 13.56 MHz with 60W was applied to the electrodes. The oxygen cylinder valve was regulated to control the flow of oxygen gas to the chamber. The cotton fibres were treated with oxygen plasma for 20 minutes.

Fig. 3.6 The experimental setup of an RF plasma system (A) Glass chamber, (B) Rotary pump, (C) Pirani gause and (D) RF generator.

Fig. 3.7 Oxygen plasma treatment process of cotton fibres.

3.2.8 Incorporation AgNPs onto cotton fibres

AgNPs were incorporated onto the cotton fibres by reducing Ag ions to AgNPs due to reducing and capping agents originating from the leaf extract. Untreated cotton fibres were weighed and immersed into the aqueous solution of AgNPs. The system was kept under constant stirring for 24 hours at room temperature. AgNPs were coated onto cotton fibres using the following steps:

Step-1: AgNPs were synthesized by adding leaf extract to the $AgNO_3$ solution. The reducing and stabilizing agents present in the leaf extract immediately reduced Ag ions to AgNPs and stabilized them.

Step-2: The oxygen plasma-treated cotton fibres were immersed into the aqueous solution of AgNPs and allowed to keep stirring for 24 hours. At that time, AgNPs were deposited onto the surface of the cotton fibres.

Step-3: Finally, AgNPs loaded cotton fibres were removed from the solution. Treated cotton fibres were washed to remove excess or loosely bound AgNPs from the surface of the cotton fibres. AgNPs incorporated cotton fibres were dried in a hot air oven at 90 ^{o}C for 3 minutes to remove the residual moisture.

The first step is crucial because the size and morphology of AgNPs were controlled during this step. The three steps discussed above are shown in the figure below.

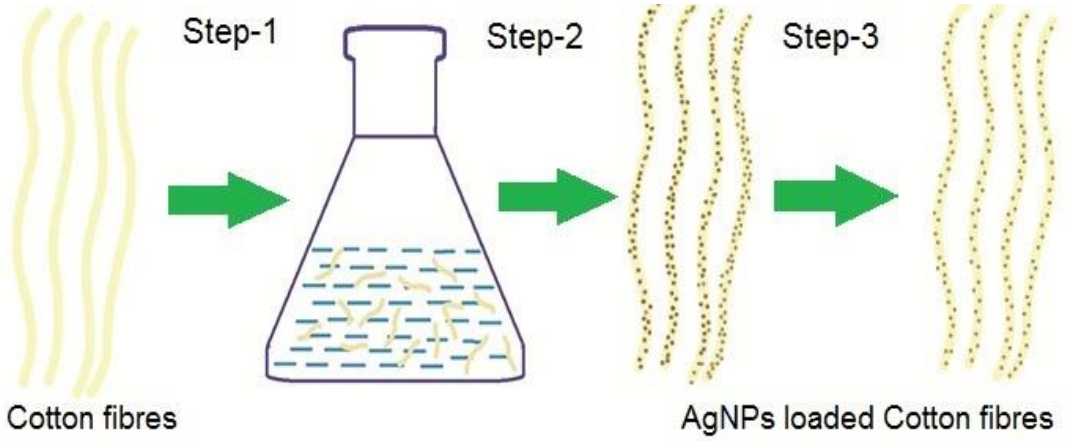

Fig. 3.8 Schematic diagram of fabrication of AgNPs incorporated cotton fibres.

3.3 Characterizations Techniques of AgNPs

The relevant techniques used to characterize AgNPs and AgNPs coated cotton fibers are described in the following sub-sections.

3.3.1 Ultra-violet visible spectroscopy

Ultra-violet visible (UV-vis) spectroscopy is an analytical technique used to measure the absorbance spectra of chemical compounds. The excitation of the electrons from the ground state to a higher energy state occurs when the molecule absorbs suitable electromagnetic radiation. The absorbed electromagnetic radiation equals the difference in the energies between the higher energy state and the ground energy state.

UV-vis spectroscopy works on the principle of Beer-Lambert law. The mathematical expression of Beer-Lambert law is-

$$A = \log\left(\frac{I_0}{I}\right) = ECl \tag{3.1}$$

Where, A = absorbance

I_0 = intensity of light incident on the sample cell

I = intensity of light leaving sample cell

E = molar absorptivity

C = molar concentration of the solute

l = length of the sample cell in cm

In this investigation, the absorbance of the bio-reduced colloidal solution of AgNPs was measured by a UV-visible spectrometer (Shimadzu Corporation, UV-2600, Japan). The spectra were taken between 200 nm and 800 nm. After adding leaf extract to the AgNO3 solution, the spectra were taken at different time intervals. And absorption spectra were also taken, varying the concentration of $AgNO_3$ salt and leaf extract

3.3.2 Fourier transform infrared spectroscopy

When a compound is exposed to infrared (IR) radiation, it selectively absorbs the radiation resulting in vibrations of the molecules of the compound. The resulting spectrum represents closely packed absorption bands, known as IR absorption spectrum.

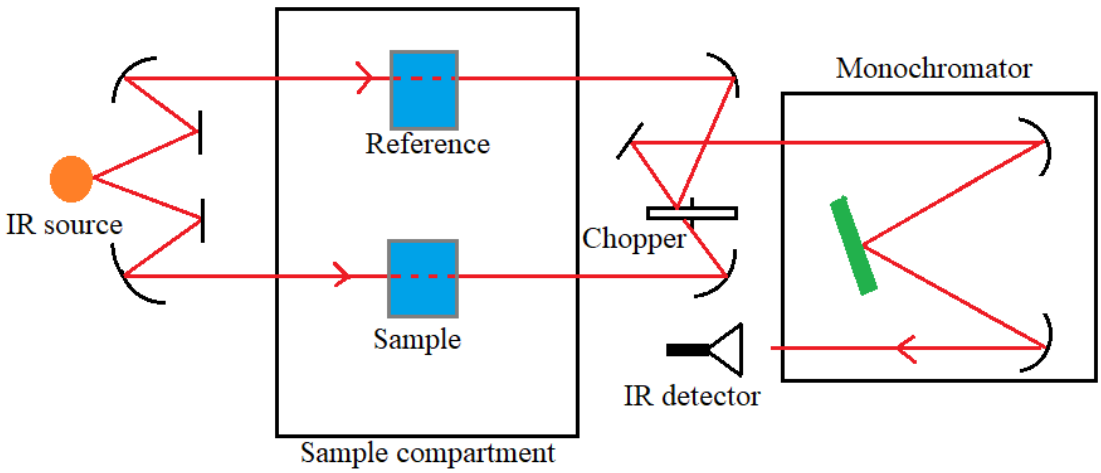

Fig. 3.9 Schematic diagram of FTIR spectroscopy.

The absorption bands correspond to the characteristic functional groups and the bonds present in a chemical substance [60]. Thus, an IR spectrum of a compound represents the molecular fingerprint for its chemical identification. An IR spectroscopy assembles the absorption information and analyzes it in the form of a spectrum by Fourier transform. The chemical composition and the functional groups present in the synthesized AgNPs were studied using an FTIR spectrometer (Shimadzu Corporation, FT-IR 8400S, Japan). FTIR spectroscopy of dried AgNPs powder was performed by using the KBr-palette technique. An appropriate quantity of KBr-palette was prepared by mixing KBr and AgNPs in a 100: 0.1 ratio. The palettes were made, taking about 100 mg of the mixture. Spectra were taken in the range from 4000 cm^{-1} to 400 cm^{-1}. The resolution of the scan was 4 cm^{-1}. The prepared palette was scanned 30 times.

3.3.3 Zeta potential measurement

The zeta potential analysis is a well-established technique that utilizes the classical theory of colloidal stability. Nanoparticles in dispersed media are electrostatically stabilized because their surfaces have additional charged species. Zeta potential was used to determine the nature and amount of that charge. It refers to the electrostatic charge density, induced near the surface of AgNPs due to the actions of ions and polymers in the suspension. Simply, it is the value of electrostatic potential on the slipping plane where the particles interact with others. The positive or negative potential indicates the type of dominant charge (negative or positive). The large positive or negative charge value indicates a strong repulsive force acting among the NPs and they will tend to repel each other, limiting the agglomeration.

The long-term stability of synthesized AgNPs was determined using Zeta potential measurement (Malvern Zetasizer). Water was used as a dispersant having a radioactive index (RI) of 1.330. Zeta potential measurement was run at 25 ^{o}C and the count rate was 362.8 pcs. It is the amount of charge developed at the interface between the surface of the solid nanoparticles and the dispersion liquid medium. It describes the cause of dispersion, agglomeration or flocculation. This measurement is applied to determine the long-term stability of nanoparticles for years.

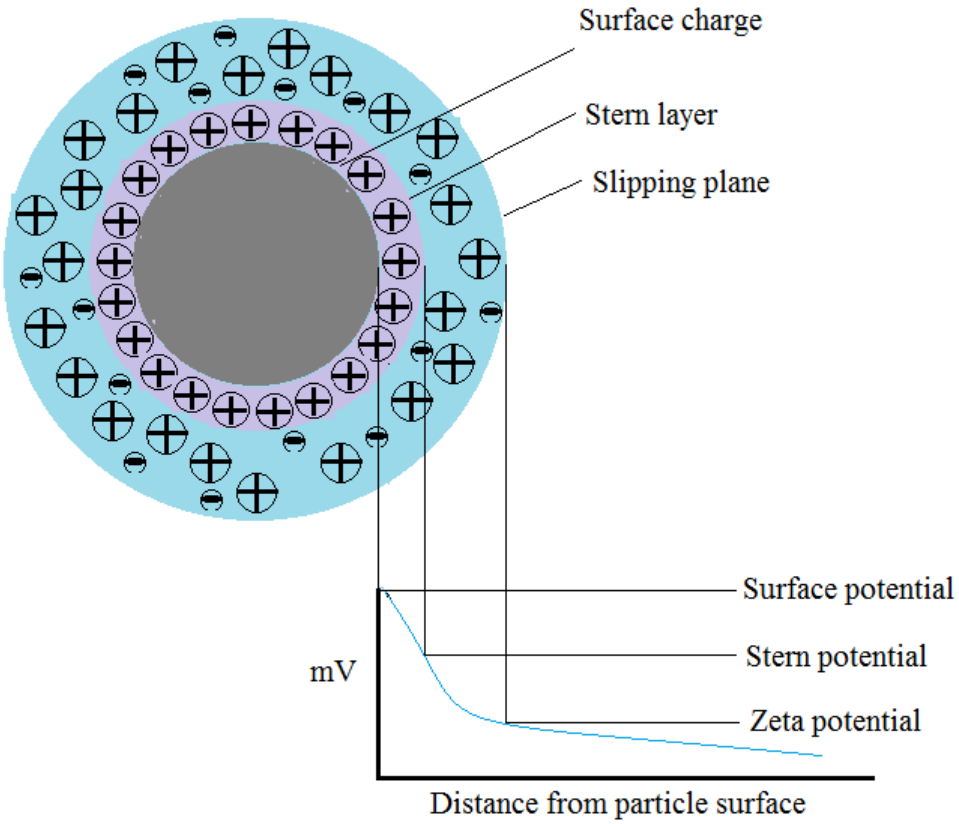

Fig. 3.10 Schematic representation of zeta potential.

Zeta potential is a physical property exhibited by most of the solid-liquid and liquid-liquid layers of the colloidal system. When nanoparticles are dispersed in a liquid medium, functional groups associated with the nanoparticles react with the dispersion medium. This reaction develops a surface charge and due to this charge, oppositely charged ions are attracted.

3.3.4 X-ray diffraction analysis

XRD is a rapid analytical technique used to study crystallographic structures. XRD peaks are produced when a monochromatic X-ray beam is scattered at particular angles from each group of lattice planes in a sample. It provides information on structures, phases, preferential crystal orientation, atomic spacing, average grain size, etc. The crystal structure and phase variation of AgNPs were studied with the help of Cu-alpha radiation at an applied voltage KV and current mA. The scan rate was degree/sec, varying 2-Theta from 10 to 90 degrees.

The crystallite size of the synthesized nanosilver was determined from the intense peak of the XRD pattern using the Scherrer's equation [61],

$$D = \frac{k\,\lambda}{\beta cos\theta} \tag{3.2}$$

D is the average crystallite size, is the wavelength of the X-ray radiation, β is the full width at half maximum (FWHM) of the respective peak in radian,n and θ is the angle of incidence in radian. K is a dimensionless shape factor whose value varies with crystalline shape and has a typical value of 0.9 [61, 62].

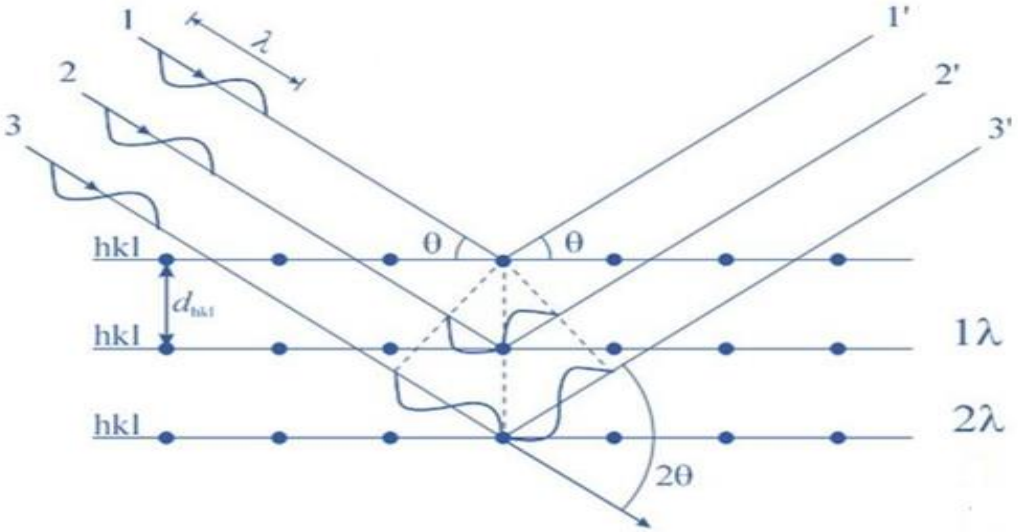

3.11 Bragg's diffraction for X-rays.

3.3.5 Field emission scanning electron microscopy

FESEM is a widely used imaging technique where electrons are emitted from a field emission source and gain acceleration in a high electrical field gradient operated in a high vacuum (10^{-4} -10^{-10} torr). These accelerated electrons are focused and deflected by electromagnetic lenses to construct a narrow scan beam that hits the object extremely fast. Consequently, secondary electrons are emitted from every spot on the object. The detector and receive these secondary electrons and produce an electrical signal. A system amplifies the signal and transforms it into a video scan image that appears on a monitor. The surface morphology, shape and size of the synthesized AgNPs were

studied using Field Emission Scanning Electron Microscope (JEOL, JSM-7600F, USA). The elemental composition of synthesized NPs was determined using Energy dispersive X-ray spectroscopy (EDS). The presence of the AgNPs on the surface of the cotton fibres was also confirmed by SEM analysis. A small amount of synthesized nano silvers and treated cotton fibres were coated with a thin carbon layer to make those conductive. Then the carbon-coated AgNPs and AgNPs incorporated in cotton fibres were characterized by FESEM at an accelerating voltage of 10 kV.

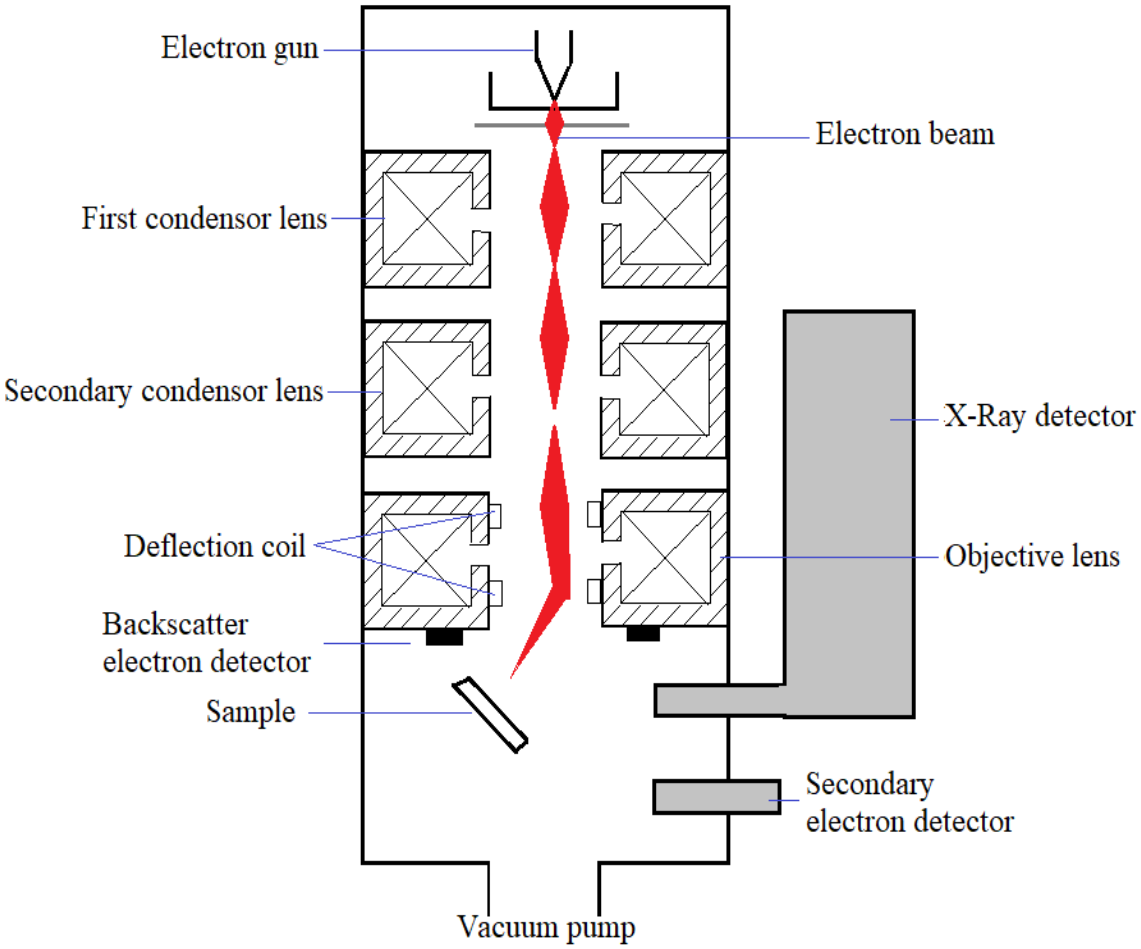

Fig. 3.12 Schematic diagram of an FESEM mechanism.

3.3.6 Transmission electron microscopy

TEM is an imaging technique where high energy (>20 keV) electron beam is focused onto the sample that produces an enlarged version to appear on a fluorescent screen or layer of photographic film. TEM can reveal the finest details of internal structure. The size and shape of the synthesized AgNPs were determined by TEM (JEOL, JEM-1400, Japan). The samples were dispersed in ethanol on a carbon-coated copper TEM grid and the samples were scanned at an operating voltage of 100 kV.

3.3.7 Thermogravimetric analysis

TGA is a thermal analytical technique that ascertains changes in physical and chemical characteristics of materials as a function of temperature. Sometimes it measures the loss of mass as a function of time with a constant temperature. TGA can provide information about physical phenomena like second-order phase transitions, such as vaporization, sublimation, absorption and desorption. The thermal stability of the synthesized AgNPs and AgNPs loaded cotton fibres was investigated by TGA using Thermogravimetric Analyzer (NETZSCH, STA-449F3). TGA was performed at temperatures ranging from 26 to 800 ^{o}C at a 10K/minute heating rate. The atmosphere was maintained under a constant nitrogen gas flow at a 40 ml/minute rate. Thermogravimetric analysis is a technique in which the mass change of substance is monitored as a function of temperature or time as the sample is subjected to a controllable temperature in a controlled atmosphere.

3.3.8 Differential scanning calorimetry

DSC is an analytical technique that measures the difference in the heat required to increase the temperature of a sample and a reference as a function of temperature. DSC can measure the amount of heat absorbed or released during transitions determining the difference in heat flowing between the sample and the reference. DSC may be used to observe more subtle phase changes. As it has application in evaluating the purity of the sample, it is widely used in industrial sectors as a quality control instrument. DSC analysis of synthesized AgNPs and cotton fibres incorporated with AgNPs was performed using a thermal analyzer (NETZSCH, STA-449F3). It was taken from 26 ^{o}C to 800 ^{o}C at a 10K/minute heating rate. Nitrogen gas at a 40 ml/minute flow rate has flowed during the measurement.

3.3.9 Antibacterial assay

The antibacterial activity of AgNPs and cotton fibres incorporated with AgNPs was investigated using the well diffusion method. The test was performed against gram-negative (*E. coli*) and gram-positive (*S. aureus*) bacteria. The bacteria were cultured on a nutrient agar plate. 25 µL of the aqueous solution of AgNPs was poured into the well on the agar media. The zone of inhibition (ZoI) was measured using photographic images of the agar plates having a clear zone around the diffusion well. The presence of a clear inhibition zone where bacterial growth was reduced was due to the antibacterial property of AgNPs. Further, AgNPs coated cotton fibres were cut into small pieces (1 cm) and kept on the cultured bacteria. The agar plates were kept under incubation at 37 °C for 24 hours and measured the ZoI to observe the antibacterial activity.

3.4 Bacteria

Bacteria are single-celled microscopic organisms that thrive in diverse environments. These organisms can live in soil, the ocean and inside the human gut. Though some bacteria are harmful, most of them serve a useful purpose, e.g., curdling milk into yogurt and helping our digestion. There are two types of bacteria depending on the stain test: gram-positive and gram-negative.

3.4.1 Gram-positive bacteria

Bacteria that give a positive result in the Gram stain test are called gram-positive bacteria. Gram-positive bacteria absorb the crystal violet stain used in the test and appear purple-colored when observed under the microscope. This is due to the thick peptidoglycan layer in the cell wall reserves the stain after washing away in the decolorization stage of the test.

3.4.2 Gram-negative bacteria

Gram-negative bacteria lose the crystal violet stain used in the gram-staining method of bacterial differentiation. The cell envelope of gram-negative bacteria comprises with a thin peptidoglycan layer. An inner cytoplasmic cell membrane and a bacterial outer membrane envelope this thin layer.

3.4.3 Kirby-Bauer antibiotic testing

Antibacterial efficiency of different antibiotics is investigated using the Agar diffusion test known as Kirby-Bauer antibiotic testing, disc or well diffusion testing. We used well diffusion method to test the efficiency of respective bacteria. In this test, an agar media was prepared in petri-dish, in which the bacteria could grow. Then synthesized AgNPs were placed into the diffusion well with typical 7 mm diameter on agar plate containing previously cultured bacteria.

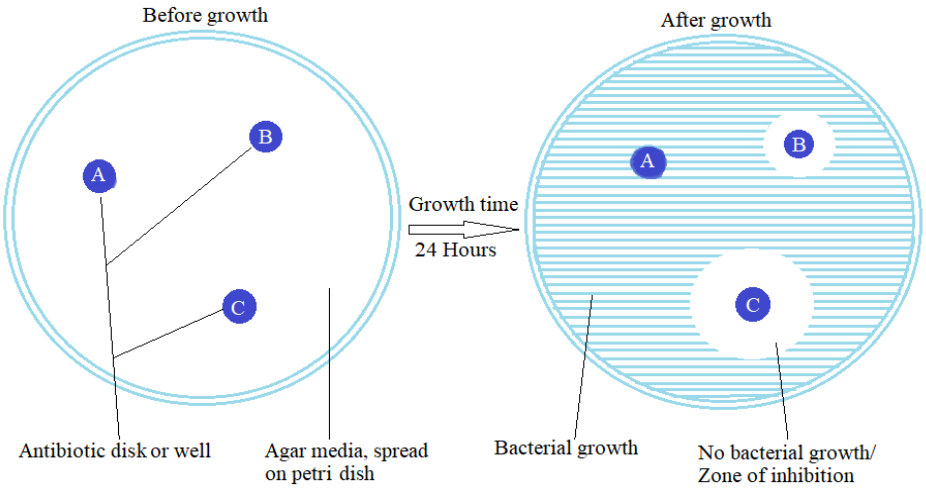

Fig. 3.13 Schematic diagram of agar disk diffusion method.

The agar plate was kept in an incubator at 37 °C for bacterial growth. If synthesized AgNPs can resist bacteria from growth or kill bacteria, there will be a clear zone around the disc or well where bacteria could not grow enough. This zone is called the zone of inhibition (ZoI).

Many factors affect the size of the ZoI, such as the effectiveness of antibiotics, diffusion of AgNPs within the agar medium, etc. The diffusion of AgNPs within an agar medium depends on the molecular concentration of the antibiotic.

The AgNPs penetrate the bacteria's cell membrane, causing damage to the lipid bilayer and bacterial death. Due to the effectiveness of AgNPs against bacteria, no colonies can grow around the well. The minimum concentration for which the ZoI can be found is

the minimum inhibitory concentration (MIC) of the AgNPs for that bacterium. ZoI produced by the NPs is analyzed with that produced by the known concentration of an antibiotic as reference. This information may help determine the appropriate concentration of AgNPs or antibiotics to fight against a particular bacterium [63]. The amount of space surrounding the well or antibiotic disks indicates how effective the antibiotic is against the bacterium. According to the Fig. 3.13, well A has exhibited no antimicrobial activity towards bacteria. Samples in B and C were effective against bacteria, where the greater ZoI for sample C shows more efficiency than that of sample B. Thus, the sample in C is highly effective, while B showed intermediate effectiveness. This technique is widely applied to identify the best antibiotic against a new or drug-resistant pathogen [64].

CHAPTER 4

RESULTS AND DISCUSSION

The optical, structural, morphological, thermal, and antibacterial properties of AgNPs and AgNPs-coated cotton fibres were determined using different characterization techniques. The results of the experimental investigations are presented below.

4.1 Visual Colour Change and UV-visible Spectroscopy

The synthesis of AgNPs occurs at room temperature. Reduction of Ag^{+} to Ag^{0} was primarily confirmed by the visual colour change of the solution. The addition of 1 ml leaf extract of *Azadirachta indica* into 10 ml of 5mM aqueous solution of silver nitrate led to the change in the colour from colourless to reddish brown, as shown in Fig. 4.1.

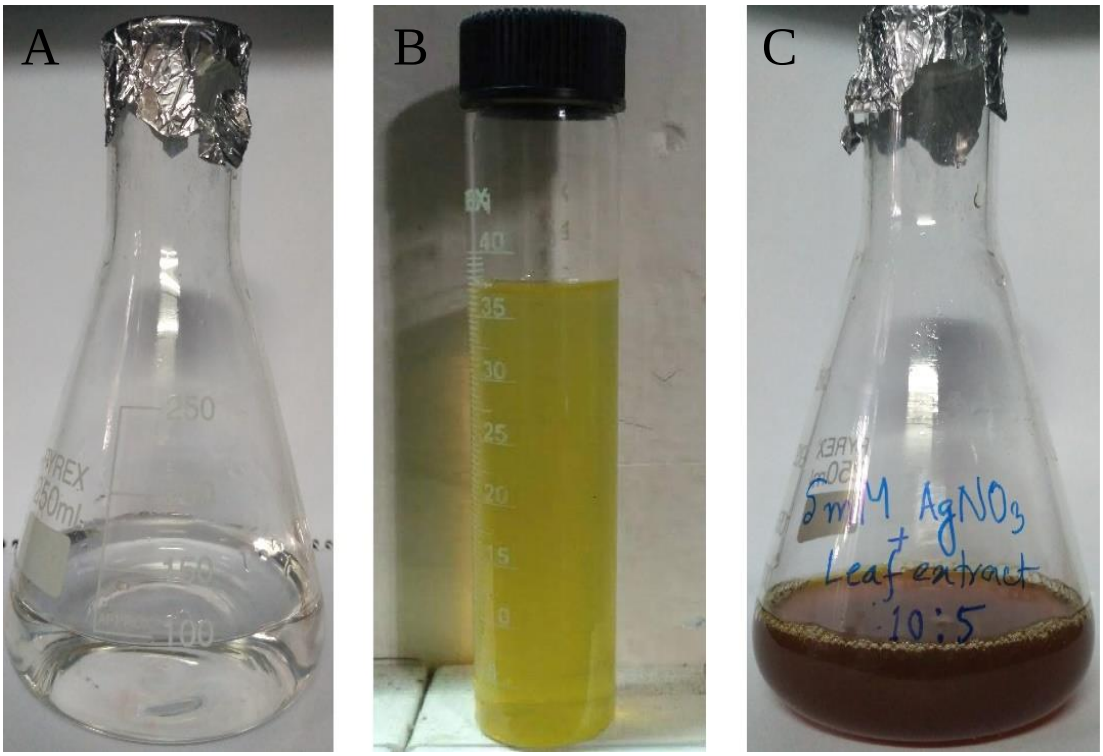

Fig. 4.1 Visual colour of (A) aqueous solution of $AgNO_3$, (B) *A. indica* leaf extract, and (C) colloidal solution of AgNPs.

The formation of AgNPs was confirmed by using UV-Vis spectroscopy. Fig. 4.2 shows the UV-Visible spectra of the aqueous solution of $AgNO_3$, *A. indica* leaf extract and colloidal solution of AgNPs, respectively. No absorption peak appeared for the aqueous solution $AgNO_3$ and leaf extract, whereas AgNPs exhibit a strong absorption peak at 438 nm due to coherent oscillations of free surface electrons of the particle, known as surface plasmon resonance (SPR) peak [65, 66]. The position of the SPR peak depends on the size, shape and distribution of nanoparticles. The SPR peak was found at 438 nm for the 10 ml of 5 mM $AgNO_3$ and 1 ml of leaf extract. The SPR bands of synthesized AgNPs are in good agreement with the literature [67, 68]. The size confinement of the conduction electron considerably influences the optical and electrical properties of metal nanoparticles.

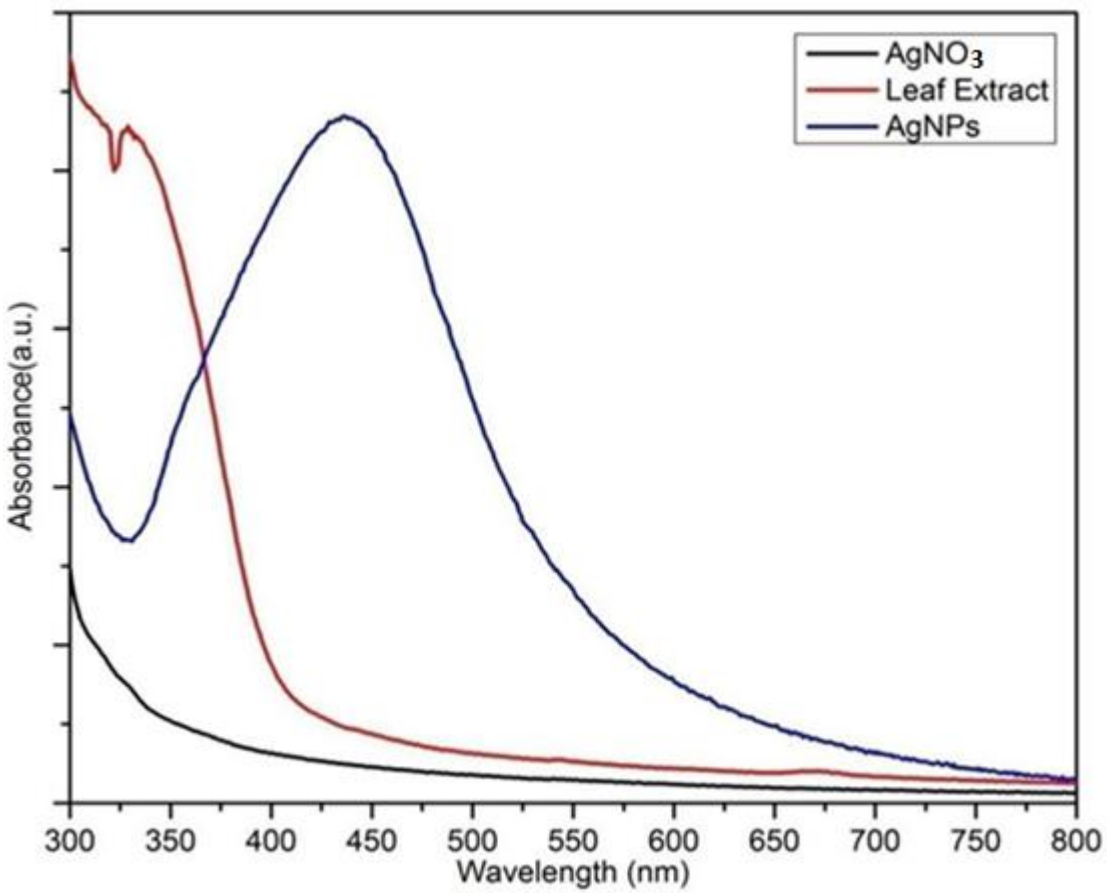

Fig. 4.2 UV-visible absorption spectra of $AgNO_3$ solution, leaf extract, and synthesized AgNPs.

In the present study, different parameters were optimized, including the concentration of silver nitrate and *A. indica* leaf extract and time. The following section discussed various parameters that were studied.

4.1.1 Effect of reaction time

The reaction was monitored at different time intervals. The colour of the silver nitrate solution changed from colourless to reddish-brown after few minutes of the leaf extract being added. Finally, the colour changed to dark brown, which confirmed the complete reduction of Ag^{+} to Ag^{0}. It took about 40 minutes to complete the reduction process. After that, no colour change was observed. Fig. 4.3 shows the effect of time on the formation of AgNPs. The visual colour change was monitored for different reaction times after adding 1 ml of leaf extract to 10 ml of 5mM $AgNO_3$ solution. Initially, at 10-20 min, the solution colour was reddish-brown; later, the colour turned to dark brown when the reaction was completed.

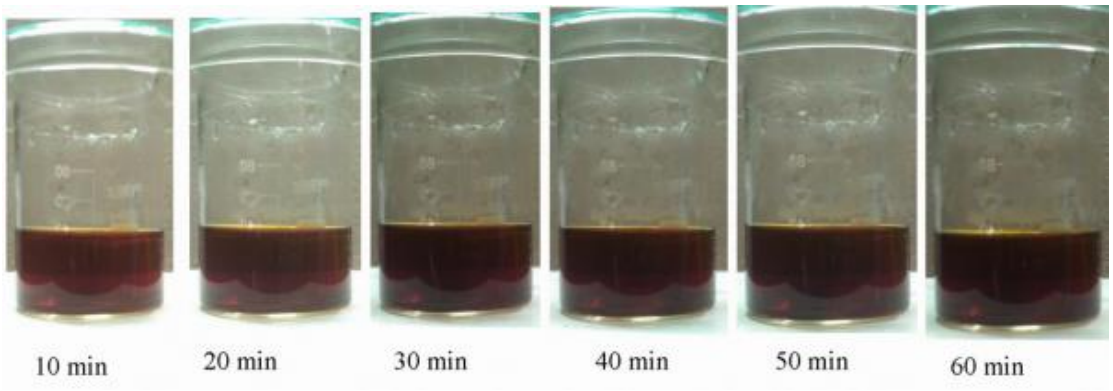

Fig. 4.3 Colour change of aqueous solution of AgNPs with time.

The synthesized AgNPs showed SPR peaks in the wavelength ranges from 438-443 nm, as shown in Fig. 4.4. SPR band depends upon the size and shape of the NPs [69]. SPR peak at wavelength ranges from 400 – 450 nm is evidence for the SPR peak of AgNPs [70].

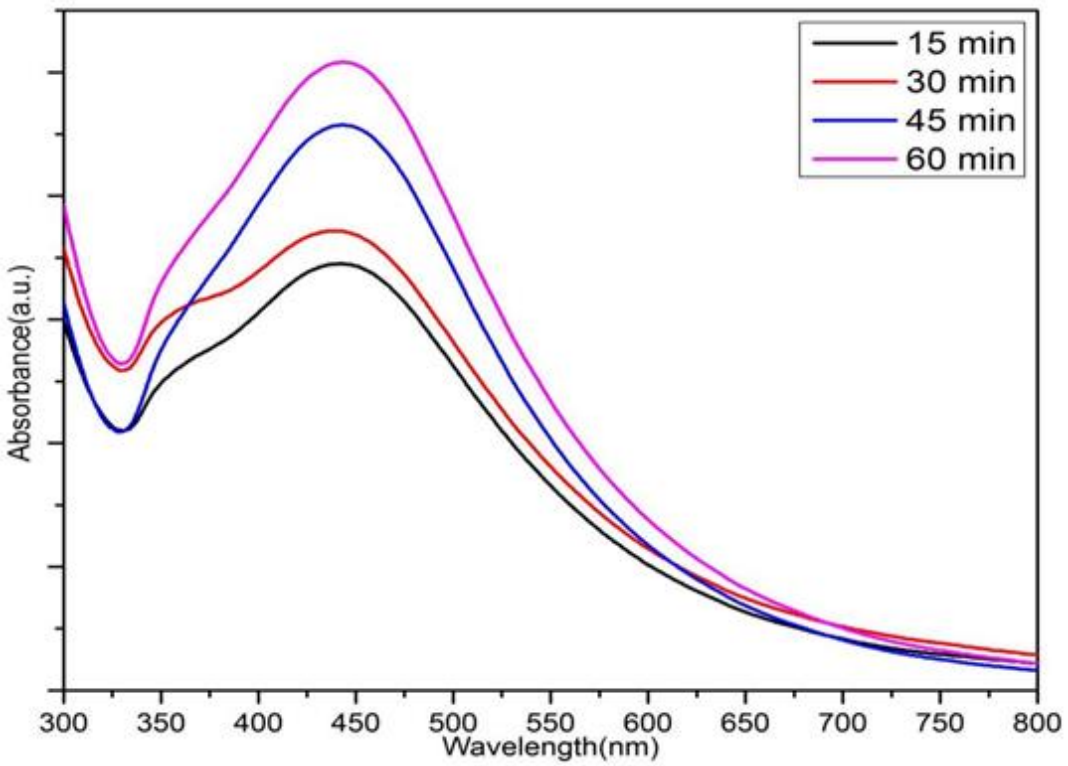

Fig. 4.4 UV-visible absorption spectra of synthesized AgNPs at different intervals using 5 mM $AgNO_3$ and leaf extract at a ratio of 10:1.

It is observed from Fig. 4.4 that the absorption intensity increased with time, indicating the number of synthesized NPs increased with reaction time. With the passage of reaction time, more Ag ions were reduced and produced a large number of AgNPs. That large number of AgNPs absorbed more UV-visible spectrum, which might be the reason that the absorption intensities increased with the increase in reaction time.

4.1.2 Effect of silver nitrate salt concentration

To study the effect of $AgNO_3$ concentration on the formation of AgNPs, different concentrations (1 mM-5 mM) of $AgNO_3$ solution were added by keeping the amount of leaf extract constant at 1 ml. Fig. 4.5 shows the visual colour of AgNPs at different concentrations of $AgNO_3$. The absorption spectra as shown in Fig. 4.6 were measured after 1 hour of reaction time. The synthesized AgNPs showed the SPR peak at 425 nm for 1 mM $AgNO_3$ solution and at 436 nm for 2-5 mM $AgNO_3$ concentrations, indicating an increase in particle size. Whereas Roy *et al.* [36] found SPR peak at 420 nm for 1 mM $AgNO_3$ solution.

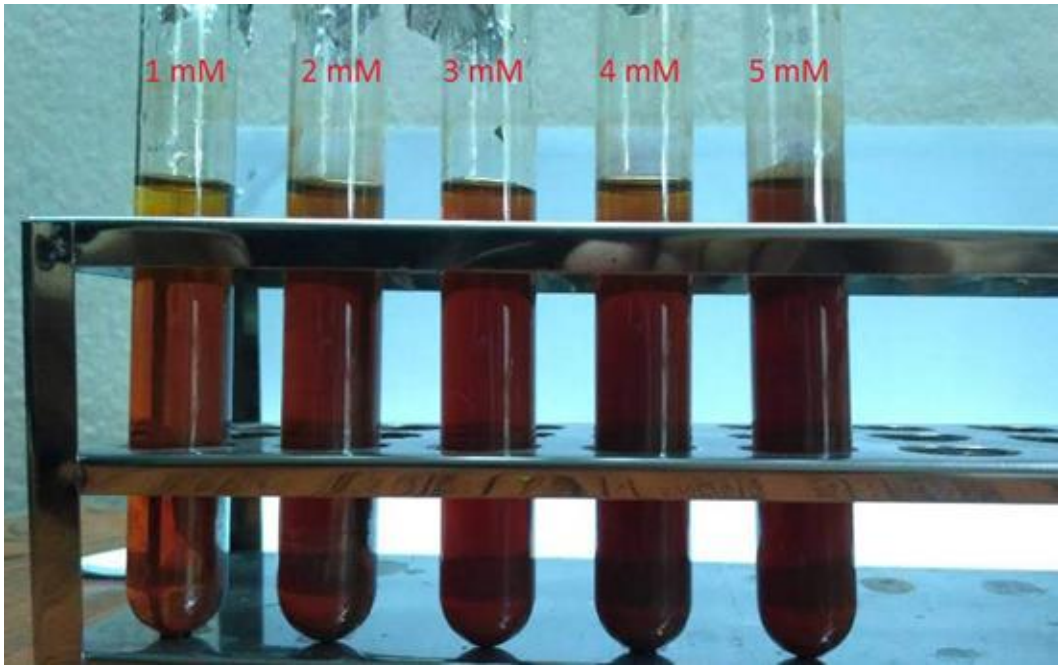

Fig. 4.5 Visual colour change at different concentrations of $AgNO_3$.

The SPR peak slightly red-shifted with time, indicating the increase in particle size [71]. The position and width of the SPR band are influenced by the size effects. With the increase in the size of AgNPs, the bandgap decreased. This narrower band gap results in a higher wavelength of electromagnetic wave emitted after the AgNPs being exposed to UV. So SPR peaks at longer wavelengths suggest the larger size of AgNPs. This size effect can also be occurred due to the confinement of conduction electrons inside the AgNPs. The decrease in bandwidth caused by the scattering of conduction electrons on the surface of AgNPs leads to an increase in the size of AgNPs [72].

In the case of increasing concentration of $AgNO_3$, the absorption intensities also increased. The more the salt concentration, the more Ag ions will be released into the solution. Consequently, the rate of reaction as well as the reduction of Ag^+ to Ag^0 accelerated with the increase of $AgNO_3$ concentration. The intensity of the SPR peak and FWHM increase with the increasing concentration of $AgNO_3$ solution. It can be concluded that the SPR peak and hence the size of NPs varied by varying the concentration of $AgNO_3$ [71].

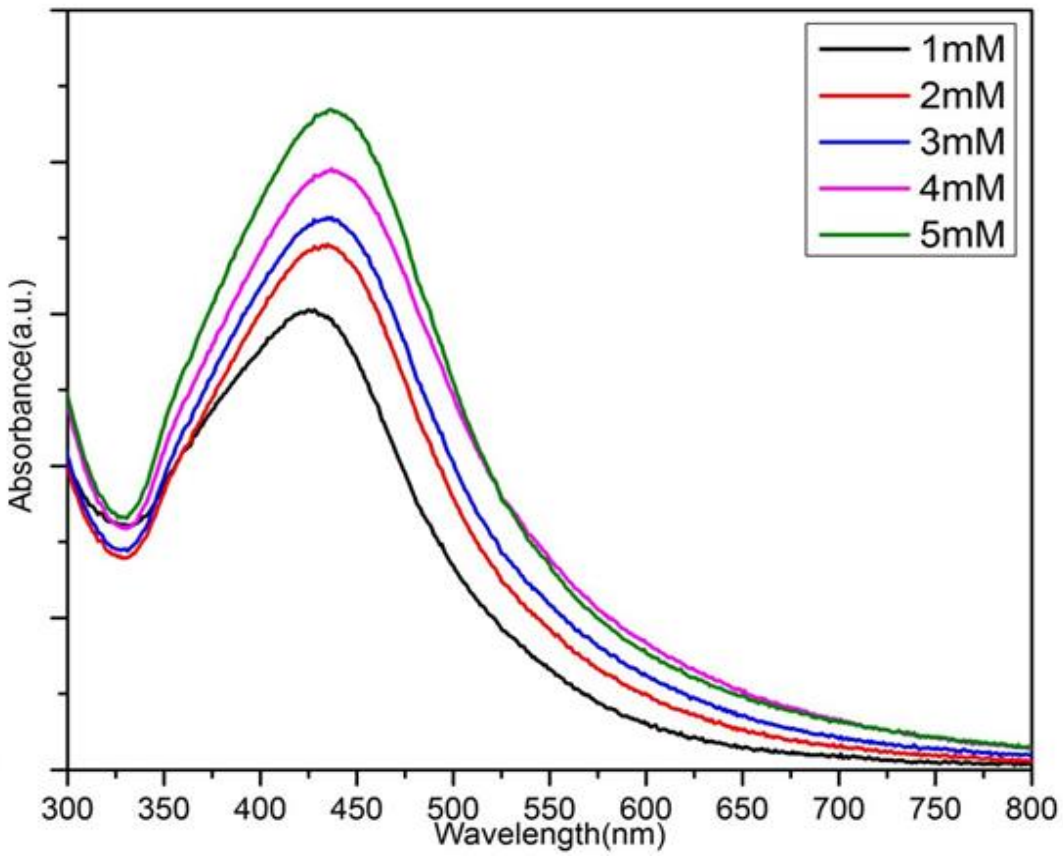

Fig. 4.6 UV-visible absorption spectra of synthesized AgNPs at different concentrations of $AgNO_3$.

When the size of NPs decreases, the number of atoms or molecules decreases. Hence, the number of overlapping orbitals decreases and the width of the valence and conduction bands get narrower. This will cause an increase in the energy gap between the valence and the conduction band. Due to this large bandgap, the movement of electrons is confined and leads to a shift of the SPR band to the lower wavelength. Therefore, a blue shift of the SPR peak suggests a decrease in NPs size, whereas a red shift indicates an increase in the size of NPs.

4.2 Fourier Transform Infrared Spectroscopy

The FTIR spectra obtained for the *A. indica* leaf powder and the synthesized AgNPs between wavenumbers 500-4000 cm^{-1} are shown in Fig. 4.7. It is observed that similar functional groups existed both in the leaf powder and the synthesized AgNPs, but their band intensities varied. These functional groups were responsible for the reduction of the Ag+ to AgNPs. These bio-molecules are also acted as the capping agent as well as the stabilizing agent.

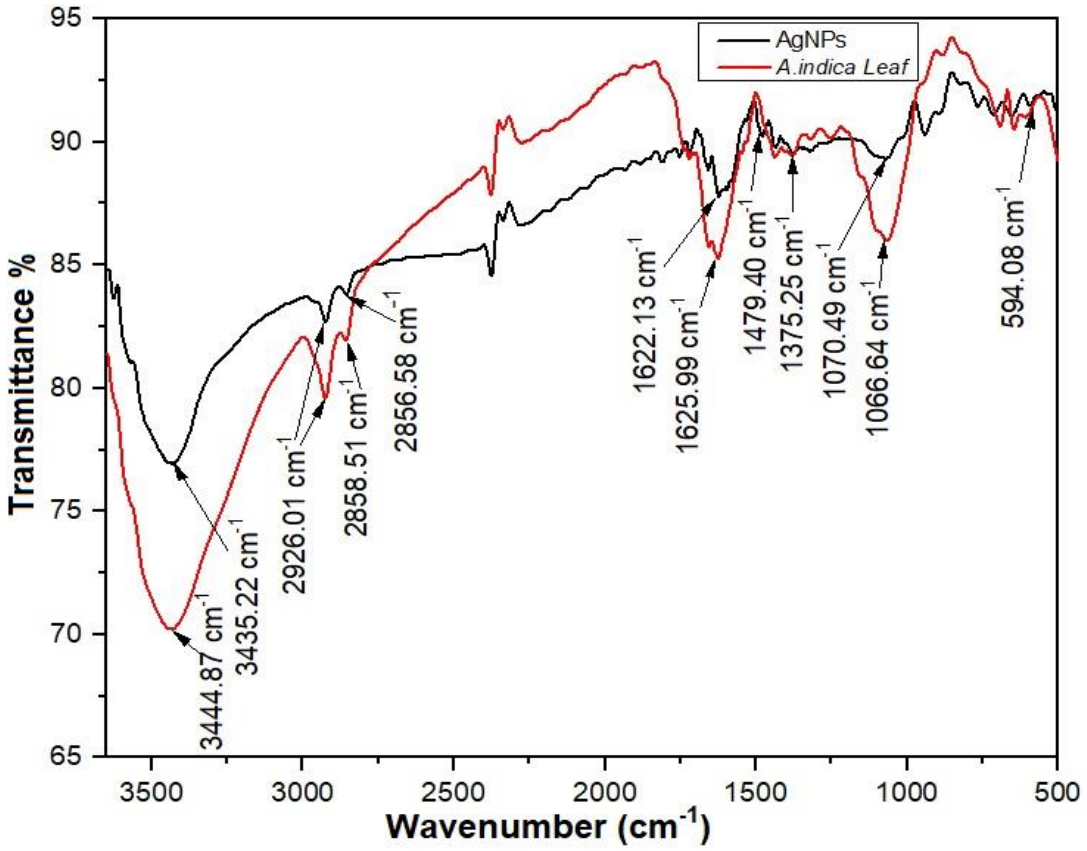

Fig. 4.7 FTIR spectra of synthesized AgNPs using 5 mM $AgNO_3$ at a ratio of 10:1 and *A. indica* leaf powder.

This spectrum has strong peaks at 3435.22, 2926.01, 2856.58, 1622.13, 1479.4, 1375.25, and 1070.49 cm^{-1} obtained for AgNPs, which is slightly shifted compared to leaf powder. Broad absorption bands at 3435.22 and 3444.87cm^{-1} of AgNPs and *A. indica* leaf powder are due to the N-H stretching vibration from the -NH_2 group and the stretching -OH vibration of the alcoholic group [67].

Thus, these absorption bands indicate the presence of H bonded alcohols and phenols. The absorption band at 2926.01 can be assigned to C-H anti-symmetric stretching vibrations and absorption peak at 2856.58 and 2858.51 cm^{-1} attributed to C-H symmetric vibration due to the functional group -CH_2. The absorption peaks at 1622.13 and 1625.99 cm^{-1} are associated with the C=C stretching vibration of alkenes in the leaf extract. Two bands at 1479.4 and 1375.25 cm^{-1} attributed to -CH bending vibrations [73].

Table 4.1 Characteristics absorptions, functional groups and attributions in FTIR of AgNPs and *A. indica* leaf powder.

Characteristics absorption (cm^{-1})		Functional groups	Attributions
A. indica leaf powder	AgNPs		
3444.87	3435.22	-OH	Stretching vibration of –OH functional group
2926.01	2926.01	$-CH_2-$	Anti-symmetric stretching vibration of $-CH_2-$ in aliphatic or naphthalic
2856.58	2858.51	$-CH_2-$	Symmetric stretching vibration of $-CH_2-$ in aliphatic or naphthalic
1622.13	1625.99	C=C	Stretching vibration of C=C in alkenes
1479.4	1375.25	CH	CH bending vibrations
1070.49	1066.64	C-O	C-O linkage in the carboxylic acid
	594.08	Ag-O	Metallic Silver

The band at 1375.25 cm^{-1} indicates the presence of flavonoids and terpenoids absorbed on the surface of the NPs. The bands at 1066.64 and 1070.49 cm^{-1} are related to the C=O linkage in carboxylic acid. The absorption band at 594.08 cm^{-1} confirmed the presence of Ag-O bond which can be attributed to the metallic silver [74].

This absorption is due to the reaction of two bio-molecules which are very plentiful in *A. indica* leaf extract. The FTIR spectra revealed that bio-molecules and functional groups responsible for reducing the Ag ions to AgNPs were released from the *A. indica* leaf extract. Carboxyl group was absorbed on the surface of the nanoparticles, which also confirmed the presence of terpenoids and flavonoids. Terpenoids and flavonoids act as capping agents for the synthesized AgNPs. Proteins and amino acids from the

carbonyl group have a strong ability to bind the NPs. Therefore these bio-molecules prevented the aggregation of nanoparticles. Thus, they stabilized the medium.

4.3 Zeta Potential Measurement

Zeta potential plays a vital role in understanding the stability of colloidal dispersion. The magnitude of this potential indicates the potential stability of the colloidal system, i.e., the degree of repulsion between the surface charge of nanoparticles in the dispersed medium [75]. In our present study, the zeta potential value was -23.2 mV, as shown in Fig. 4.8. The negative zeta potential value of the AgNPs may be due to the potential capping of the bioorganic components present in the leaf extract.

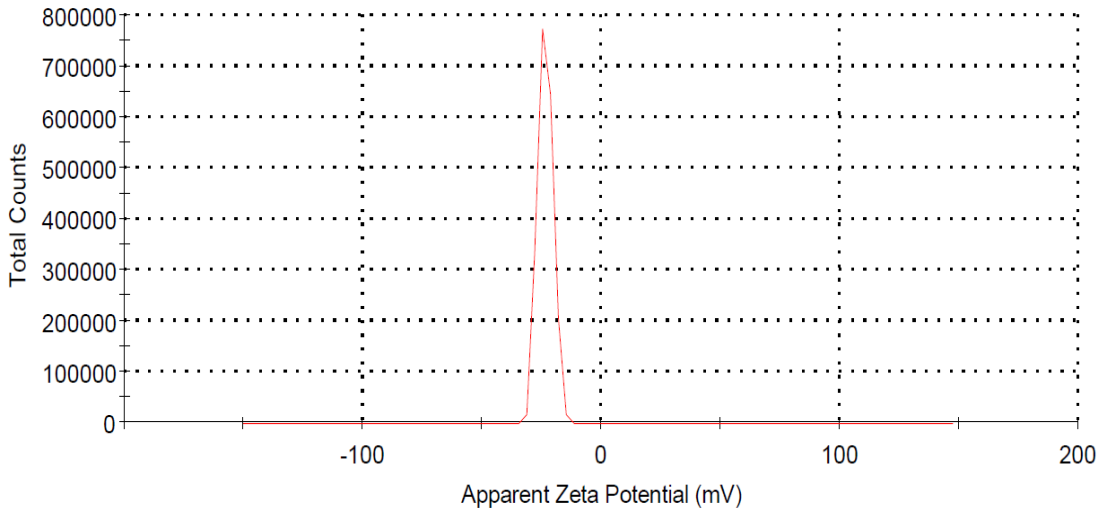

Fig. 4.8 Zeta potential measurement of synthesized AgNPs using 5 mM $AgNO_3$.

The high negative value revealed the electrostatic repulsion between the nanoparticles, i.e., synthesized nanoparticles remained apart from each other. It indicates that this potential prevented AgNPs from agglomeration and provided stability to NPs in the solution. The value of zeta potential from -20 mV to -30 mV, is considered moderately stable [76]. The large negative potential value may be arisen due to the capping by polyphenolic constituent originating from the leaf extract [77, 78].

4.4 X-ray Diffraction Analysis

The crystal structure and different structural parameters of the synthesized AgNPs were analyzed by XRD spectrum. Fig. 4.9 shows the XRD pattern of biosynthesized nanosilver by using *A. indica* leaf extract. The XRD result showed distinct diffraction peaks at angles 2θ equal to 38.02°, 44.23°, 64.43°, 77.37° and 81.59°. These peaks correspond to the (111), (200), (220), (311), and (222) planes, respectively. These lattice planes are well-matched with standard JCPDS card no. 04-0783 and confirmed that the nanosilver possesses a face-centered cubic crystal structure with preferential orientation along the (111) plane [79-81]. Therefore, the XRD pattern shows that the synthesized AgNPs are polycrystalline in nature.

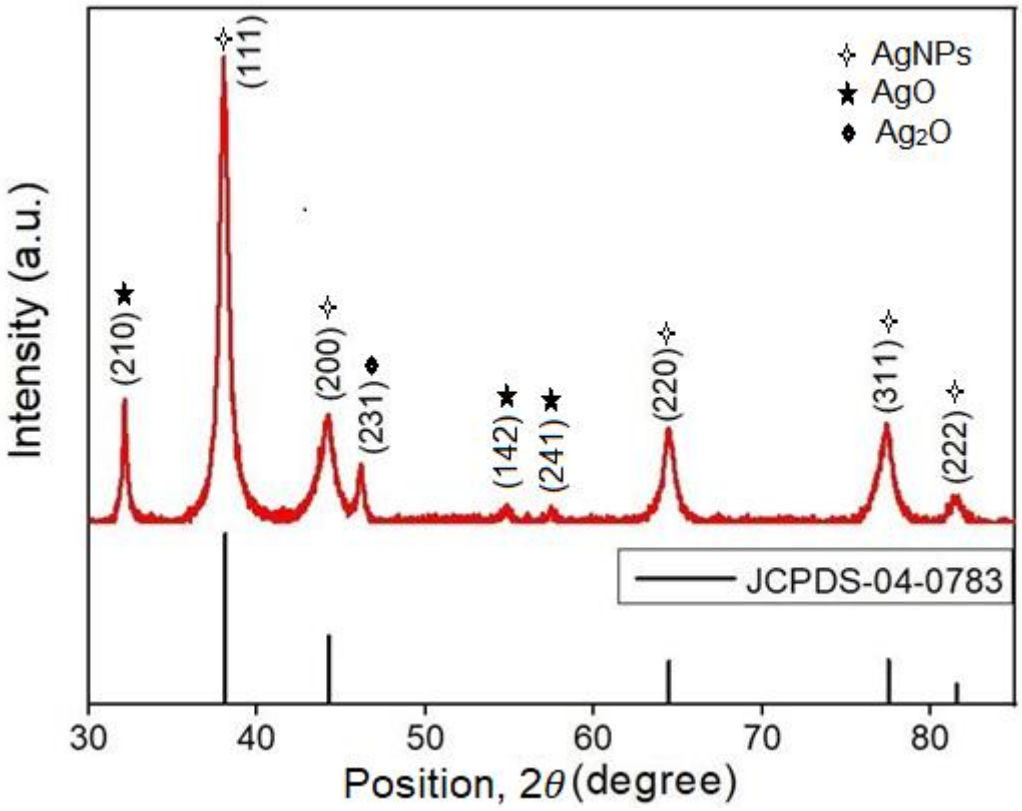

Fig. 4.9 XRD pattern of synthesized AgNPs using 5 mM $AgNO_3$ at a ratio of 10:1.

The smaller peaks are also observed at angles 32.13°, 46.19°, 54.99° and 58.63° corresponding to the planes (2 1 0), (2 3 1), (1 4 2) and (2 4 1), respectively. These planes are well-matched with standard JCPDS card no. 84-1108 and 42-0874. These

planes are possibly due to the plant bioactive compounds like AgO (Ag^{3+}) and Ag_2O (Ag^{+}), respectively [79, 82]. These peaks are weaker than those of AgNPs. During the stabilization of AgNPs, Ag^{+} was got wrapped into AgNPs. Ag^{+} exists either in a complex form or can be adsorbed onto the biomolecules. On the other hand, Ag^{3+} was due to the oxidation of Ag^{+} or Ag^{3+} was protected to exist in AgNPs. Ag^{3+} are very stable and they also might exist in a complex form and are attached to AgNPs. Earlier researchers reported similar results and mentioned that it might be due to the bioorganic compounds coated on the surface of AgNPs [80, 83]. The average crystallite size and the lattice constants of the biologically synthesized AgNPs were calculated by Scherrer's equation [61].

The average size and the lattice constants of the synthesized AgNPs are displayed in the table below:

Table 4.2 Structural parameters of synthesized AgNPs obtained from XRD pattern

Position 2θ (Degree)	FWHM (degree)	Interplanar spacing (nm)	Plane (h k l)	Crystallite size (nm)	Lattice parameter, a (nm)
38.02	0.4093	0.238	1 1 1	20	0.4095
44.23	0.4093	0.205	2 0 0	21	0.4092
64.43	0.3582	0.145	2 2 0	26	0.4086
77.37	0.5117	0.123	3 1 1	20	0.4089
81.59	0.8187	0.118	2 2 2	13	0.4096

Table 4.2 shows various structural parameters. The average crystallite size was calculated ~20 nm. The lattice parameter deviated slightly nearly consistent with the standard value of 0.4086 nm (JCPDS-04-0783). Table 4.2 also shows that the size of AgNPs decreases with the increasing FWHM, which strongly supports the Mie theory [84].

4.5 Field Emission Scanning Electron Microscopy

The surface morphology and shape of the synthesized AgNPs were observed by investigating FESEM images. The presence of AgNPs on the surface of the cotton fibres was also confirmed by FESEM analysis. FESEM micrographs revealed that the synthesized AgNPs were spherical in shape and were nearly uniform in size distribution.

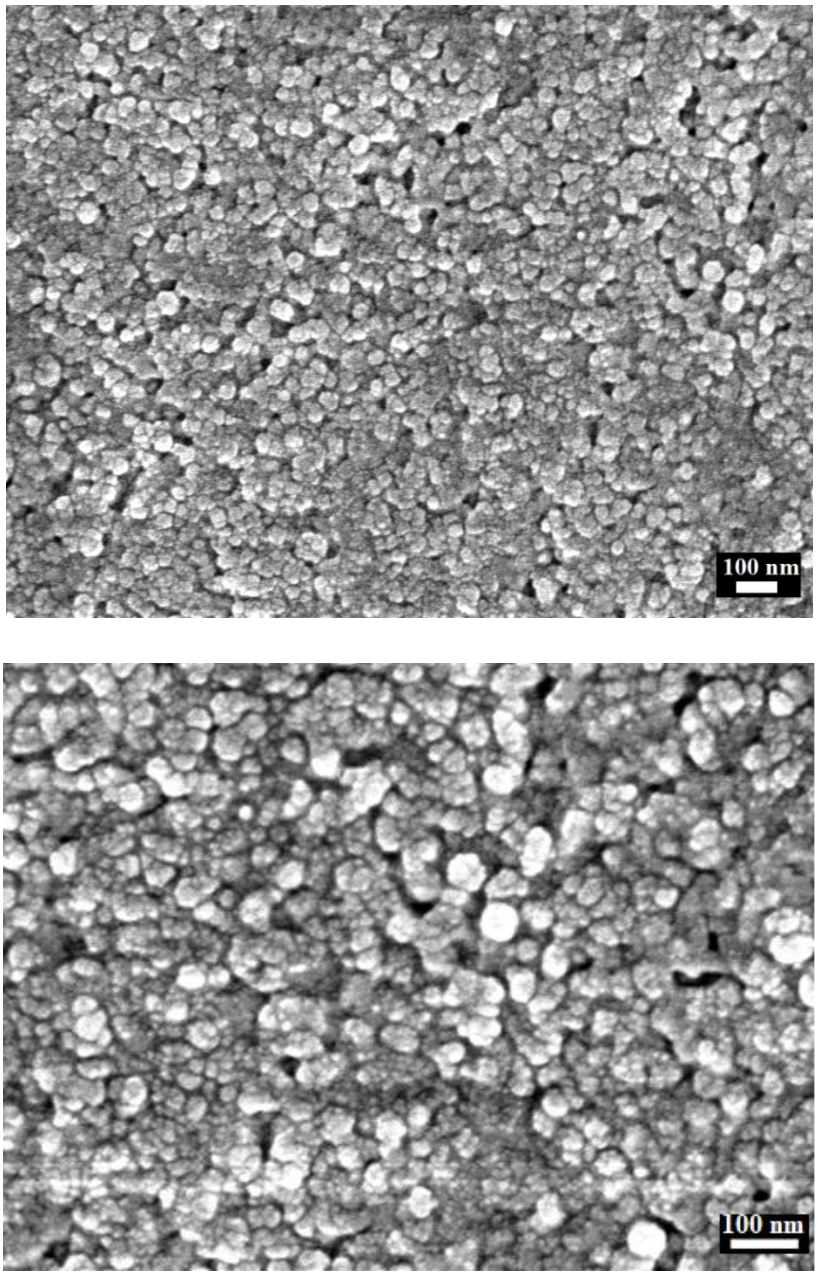

Fig. 4.10 FESEM images of AgNPs for 5mM $AgNO_3$ solution and leaf extract at a ratio of 10:1. The bottom image is the magnified version of the top one.

The size of the nanoparticles is slightly larger than the actual size of the nanoparticles because they were coated with proteins and other functional groups. Fig. 4.10 shows the micrographs of synthesized AgNPs in the case of 5mM $AgNO_3$ and leaf extract at a ratio of 10:1. The size and shape of the synthesized AgNPs varied as seen from the different magnifications. The FESEM image also shows that most AgNPs are well dispersed and some are aggregated. This aggregation occurred when the liquid containing AgNPs was evaporated on a flat surface and the NPs were coagulated along the outer edges. Nevertheless, this synthesis process is highly applicable to produce nano-size silver.

The particle size distribution for this condition was calculated using ImageJ software. The histogram (Fig. 4.11) shows the size distribution of AgNPs synthesized by taking 5 mM $AgNO_3$ solution and leaf extract at a 10:1 ratio. The histogram shows that maximum AgNPs have sizes ranging from 15 nm to 25 nm. The size of NPs is nearly matched with the crystallite size calculated from the XRD pattern.

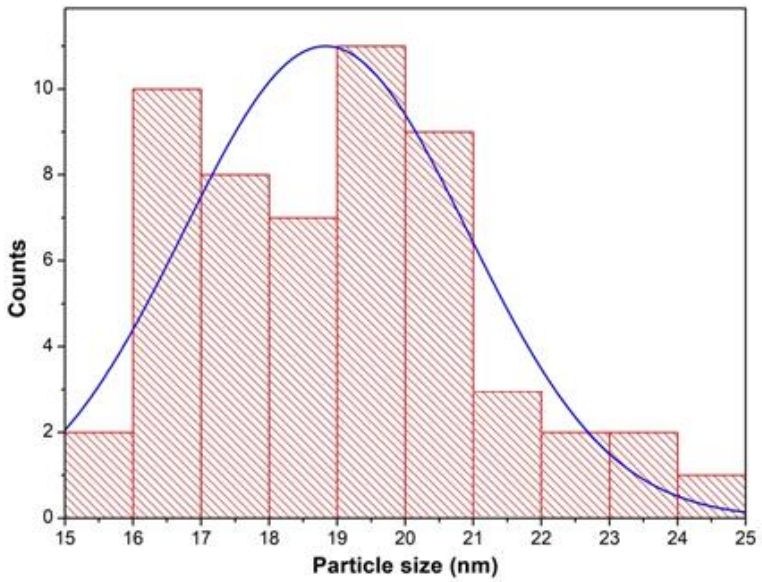

Fig. 4.11 Particle size distribution of AgNPs for 5mM $AgNO_3$ leaf extract at a ratio of 10:1.

Fig. 4.12 shows an image of AgNPs synthesized by taking 5 mM $AgNO_3$ and leaf extract at a ratio of 10:5. In this condition, it is seen that different sizes AgNPs have formed. The size of AgNPs was slightly larger for the increasing ratio of leaf extract. Slightly

larger particles may be formed due to the excess amount of biomolecules that can be attached to the surface of AgNPs. FESEM micrographs also showed that particles formed less agglomeration with the increasing concentration of leaf extract. The reason might be an adequate amount of reducing agent provided by leaf extract. The synthesized nanoparticles are nearly equal in shape and size. Therefore, AgNPs synthesized with this condition are well dispersed, have nearly uniform shape and size, and have less agglomeration.

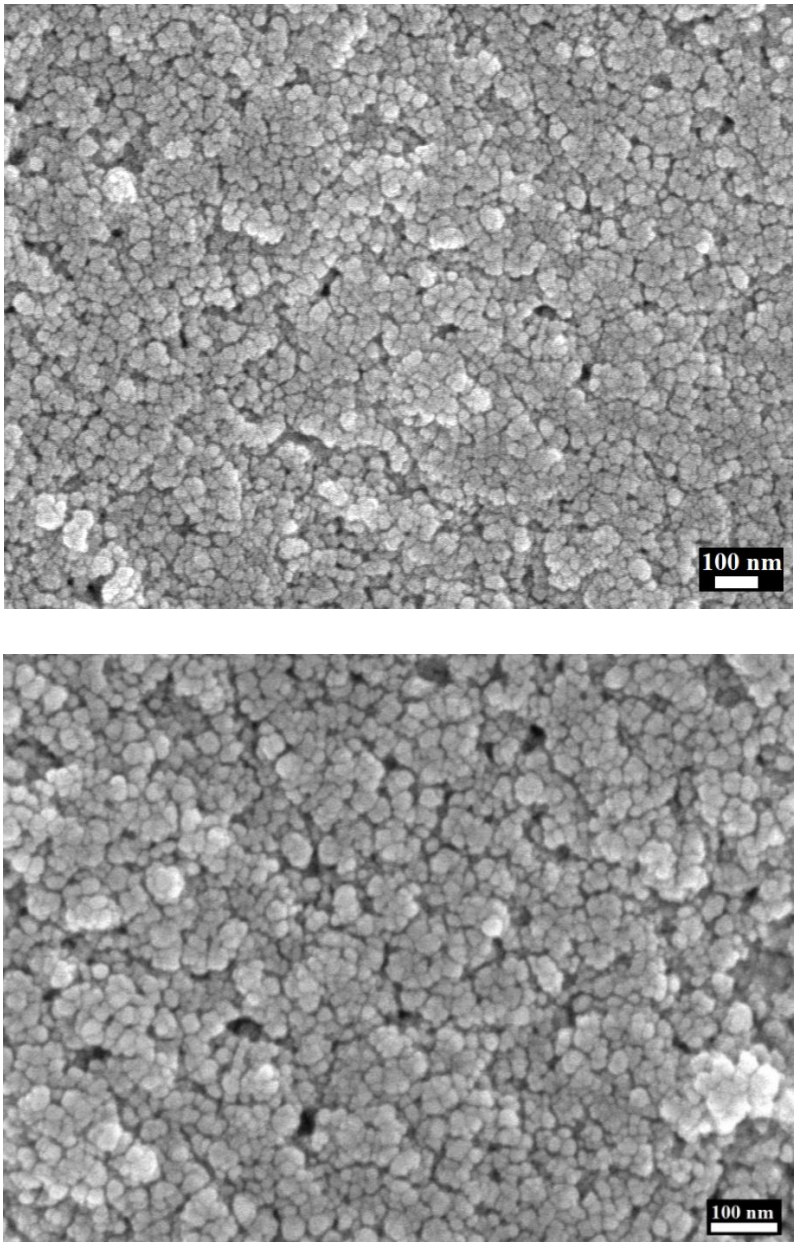

Fig. 4.12 FESEM image of AgNPs for 5 mM $AgNO_3$ solution and leaf extract at a ratio of 10:5.

Fig. 4.13 provides the histogram, which shows that particle size is distributed in 18 to 22 nm. The Gaussian curve suggests that synthesized AgNPs have narrow size distribution. Further study should be needed to investigate the effect of leaf extract concentration on the shape and size of synthesized AgNPs. Dispersion stability should also be tested to investigate whether AgNPs synthesized using this condition are more or less stable.

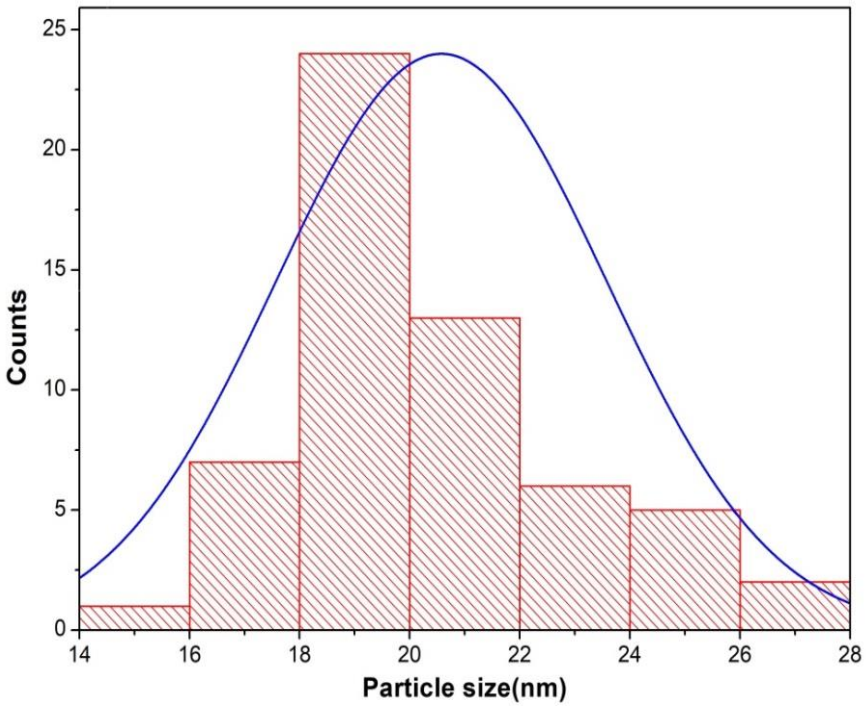

Fig. 4.13 Particle size distribution of AgNPs for 5mM $AgNO_3$ and leaf extract at a ratio of 10:5.

Particle size is strongly dependent on the molarity of $AgNO_3$ salt. Concentration also plays a vital role in determining morphology as well as affects the rate of reaction largely. Fig. 4.14 shows the shape and surface morphology of synthesized AgNPs taking 10 mM $AgNO_3$ solution and leaf extract at a ratio of 10:1. The size of AgNPs is relatively larger than that obtained for the conditions above. The size distribution of the AgNPs shows that the diameter varies from 45 nm to 75 nm for 10 mM $AgNO_3$ and leaf extract at a ratio of 10:1. This result is consistent with the result obtained from UV-vis spectroscopy. This may be due to the excessive amount of Ag^+ and fewer reducing and stabilizing agents. As the ratio of $AgNO_3$ was much more than that of leaf extract, less

amount of biomolecules were unable to stabilize the synthesized AgNPs. This resulted in the aggregation of AgNPs, which caused larger-sized particles.

But FESEM micrographs of 10 mM $AgNO_3$ and leaf extract at a 10: 1 ratio confirmed that synthesized AgNPs are larger in size but have a spherical shape and uniform distribution. So this condition can be applied to synthesizing nanoparticles of larger size. Nevertheless, the particle size distribution of AgNPs synthesized using 5 mM $AgNO_3$ is nearly equal to that obtained from XRD data.

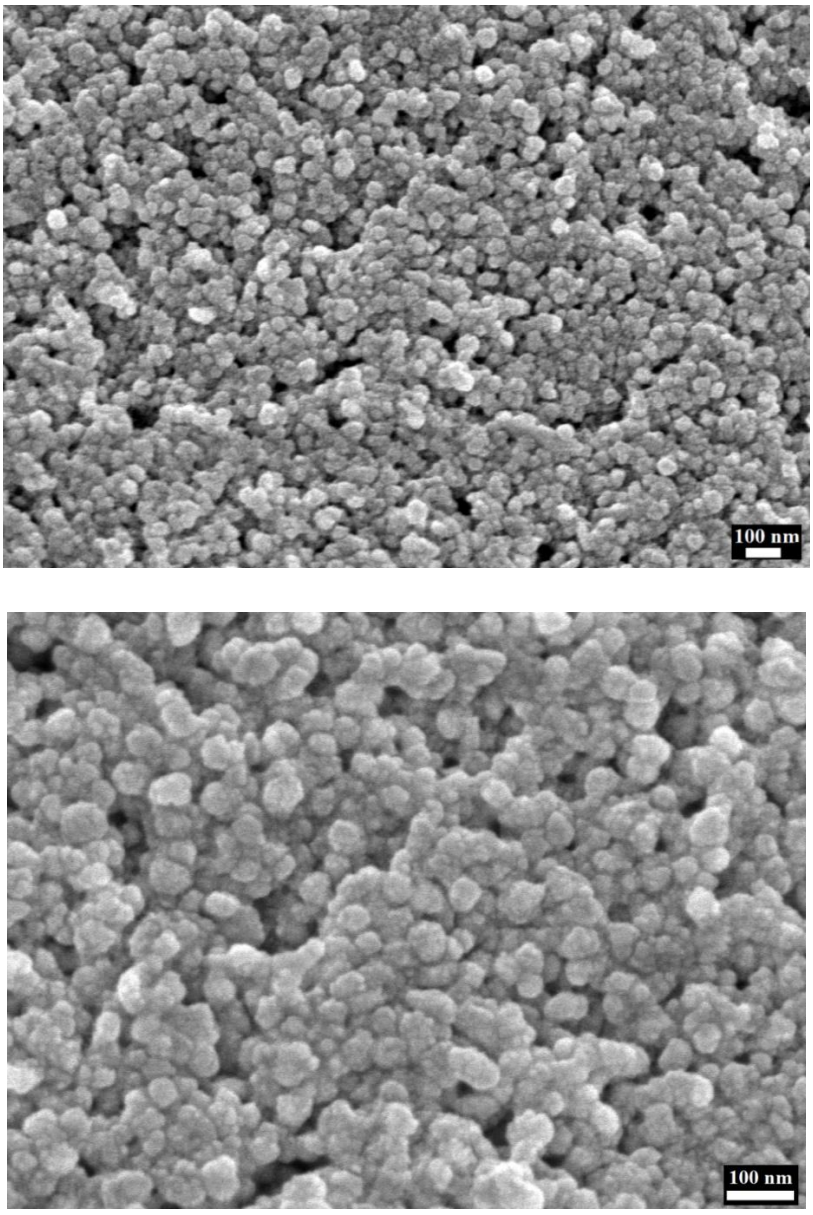

Fig. 4.14 FESEM images AgNPs for 10 mM $AgNO_3$ solution and leaf extract at a ratio of 10:1.

Gaussian distribution of the histogram revealed that AgNPs having size ranges from 50 to 55 nm were dominating.

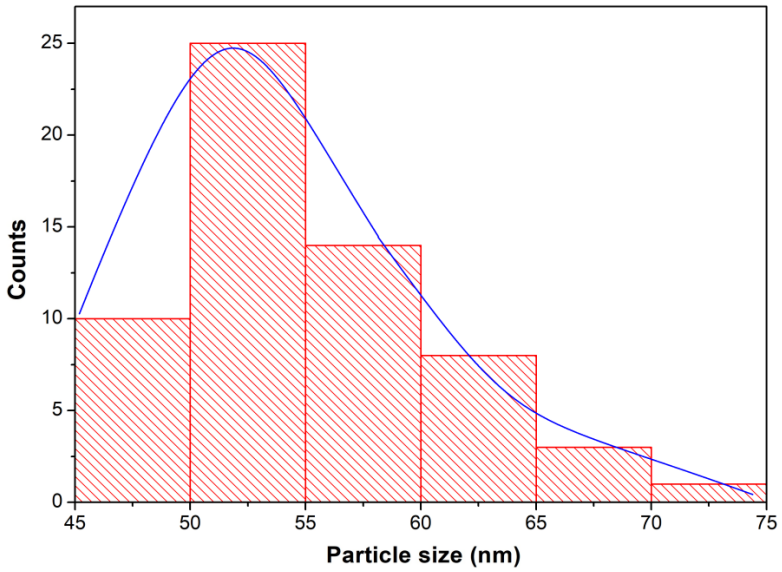

Fig. 4.15 Particle size distribution of AgNPs for 10 mM $AgNO_3$ and leaf extract at a ratio of 10:1.

Another goal of the present study was to incorporate the biologically synthesized AgNPs onto the cotton fibers to prepare antibacterial cotton fibers for practical application in the biomedical field. FESEM micrographs revealed that AgNPs were well attached to the cotton fibres.

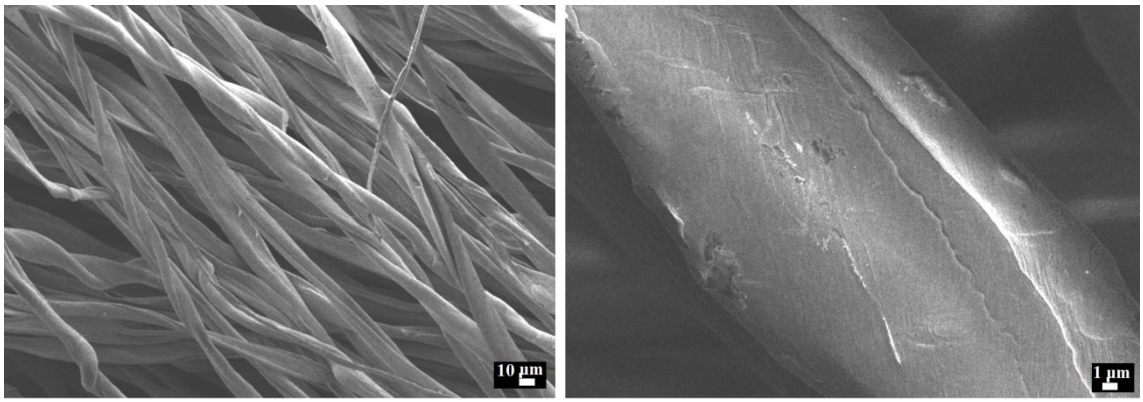

Fig. 4.16 FESEM images of control cotton fibers at different magnifications.

Fig. 4.16 present FESEM images of control cotton fibres at two different magnifications. Control cotton fibres exhibit smooth surface. The FESEM image at higher magnification demonstrated that the surface of the cotton fibres is clean and smooth. Some cracks were also seen from higher magnification images, which may be due to the stress when coated with carbon.

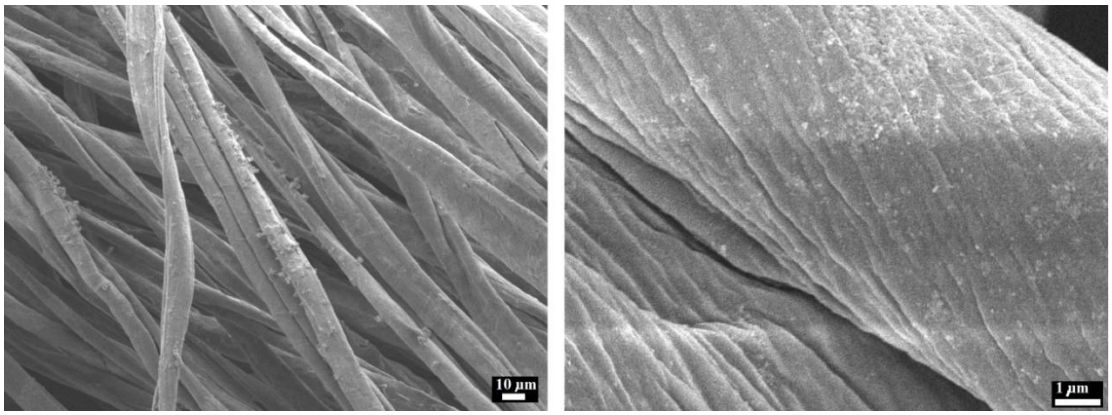

Fig. 4.17 FESEM images of AgNPs coated cotton fibers at two different magnifications.

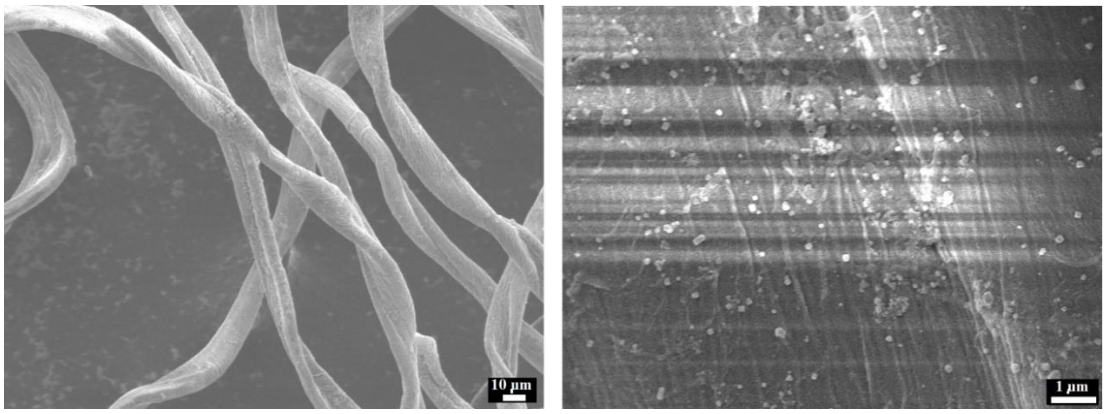

Fig. 4.18 FESEM images of AgNPs incorporated plasma-treated cotton fibres at two different magnifications.

Fig. 4.17 showed the FESEM images of AgNPs coated cotton fibres at two different magnifications. This image exhibited the presence of AgNPs on the surface of the cotton fibres. Cotton fibres were scanned at higher magnification for a better view.

FESEM images revealed that the incorporated AgNPs were smaller in size and were well attached all over the surface of cotton fibres.

Fig. 4.18 showed FESEM images of AgNPs coated oxygen plasma-treated cotton fibres. After surface modification by oxygen plasma treatment, cotton fibres became free from impurities such as oily and waxy substances. Moreover, alkali treatment before the oxygen plasma treatment reduced cellulosic substances from the surface of cotton fibres. This made the cotton fibres more hydrophilic and due to the oxygen species AgNPs were more attracted to the surface. The surface morphology showed that treated cotton enhanced surface roughness. By comparing the above images, we can see that the later shows more AgNPs on the surface than the earlier. So the possibility of deposition of AgNPs onto the cotton fibres increased after plasma treatment. This surface roughness or plasma etching appeared due to the bombardment of plasma species and AgNPs were uniformly attached to the surface of the cotton fibres. In higher magnification of FESEM images, the black and white stripes may be due to the charging effect.

4.6 Energy Dispersive Spectroscopy

EDS analysis illustrated the compositional analysis of synthesized AgNPs using *A. indica* leaf extract. The AgNPs were coated with carbon and examined for EDS. Since AgNPs were synthesized using *A. indica* leaf extract and $AgNO_3$ solution, it could not be said that synthesized AgNPs have silver atoms as only constituents. The biomolecules from leaf extract also may contribute to the AgNPs.

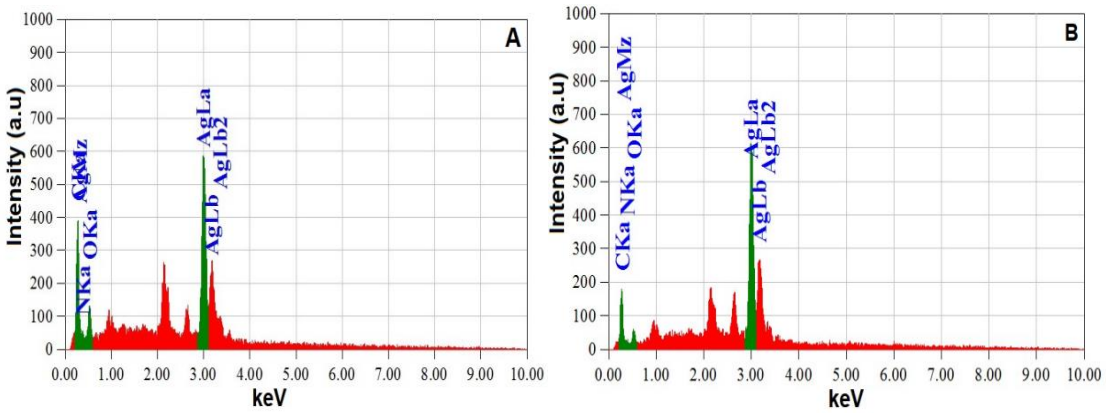

Fig. 4.19 EDS spectra of AgNPs synthesized using 5 mM $AgNO_3$ and leaf extract at (A) ratio 10:1 and (B) ratio 10:5.

Fig. 4.19 shows the elemental composition of synthesized AgNPs. EDS spectrum suggests that the majority of the constituents atom is silver. The intense peak at 2.98 keV strongly confirmed the presence of nanocrystalline elemental silver, as it has optical absorption in this range due to the SPR.

Silver exhibits optical absorption at 3 keV due to SPR [85]. The other composition elements (C, O and N) belonged to plant extract and $AgNO_3$, which confirmed the presence of different functional groups that capped the AgNPs. The signatures of C and O might be from the protein, which acted as a stabilizing agent. The total result was tabulated in Table 4.3.

Table 4.3 EDS analysis of synthesis AgNPs

Composition	Type	Ag	O	C	N
A	Mass%	71.65	9.93	15.14	3.29
	Atomic%	23.89	22.32	45.35	8.44
B	Mass%	84.87	4.93	7.96	2.24
	Atomic%	41.03	16.07	34.57	8.32

4.7 Transmission Electron Microscopy Analysis

Since the NPs possess unique physical and chemical properties depending on their shape and size, the shape and size distribution of AgNPs is a crucial issue. So it is important to carry out the synthesis method, which provides uniformly sized and shaped AgNPs. The shape and size of the synthesized AgNPs were examined by using TEM. Fig. 4.20 revealed that the synthesized AgNPs are spherical shaped. TEM images were obtained for $AgNO_3$ salt concentrations of 1 mM and 5 mM, respectively**.** TEM micrographs of synthesized AgNPs revealed the presence of a capping layer around the AgNPs, where the leaf extract provided the capping layers. These capping layers have an important role in the size distributions of AgNPs. The exploitation of *A. indica* leaf extract not only played a role as a reducing and capping agent but also enhanced the antibacterial properties of synthesized AgNPs. From our study, the biosynthesized

AgNPs showed a nonuniform size and shape for 5 mM $AgNO_3$ solution. The TEM micrographs also suggested that particle size increased with the increase in the concentration of $AgNO_3$.

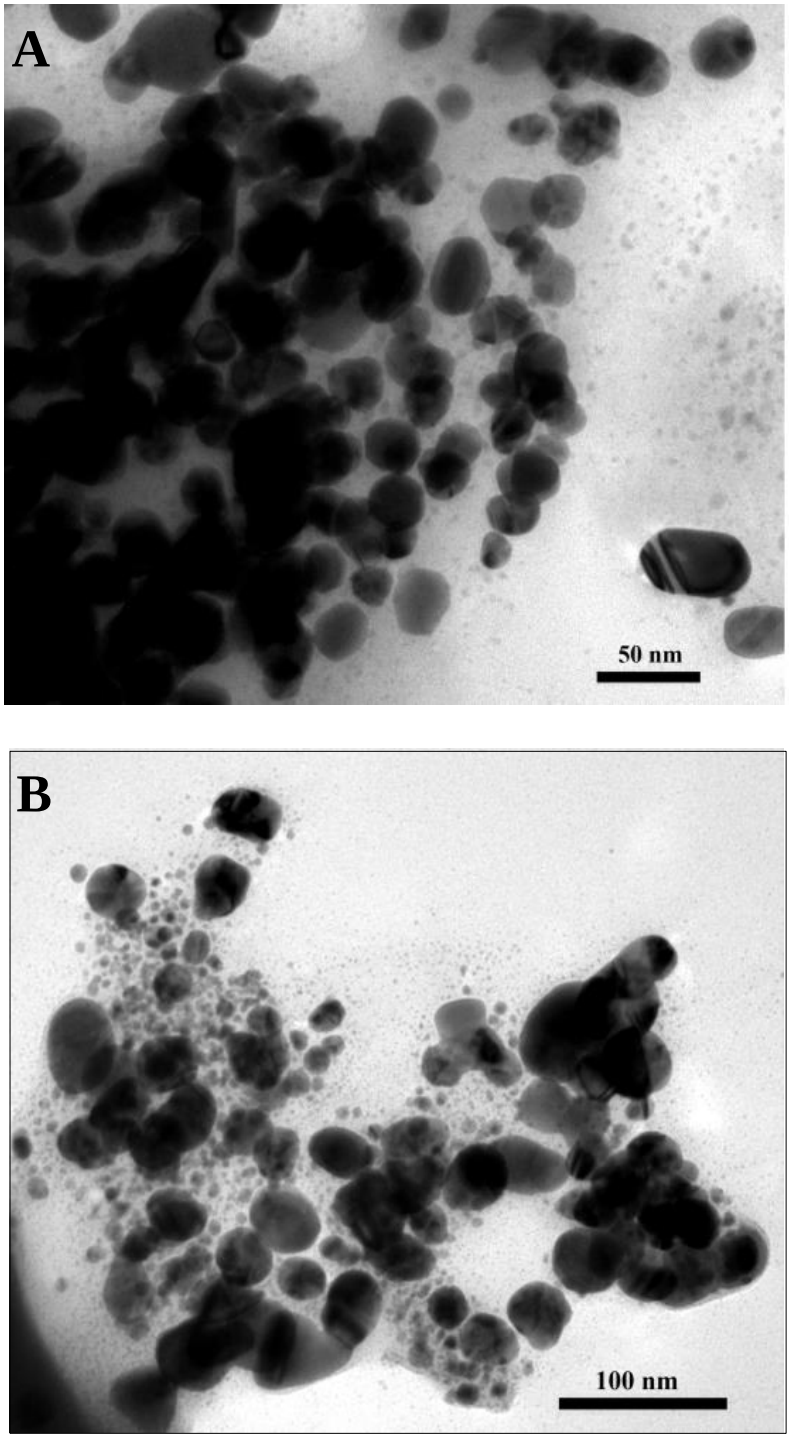

Fig. 4.20 TEM micrographs of the synthesized AgNPs (A) 1 mM (B) 5 mM $AgNO_3$ solution.

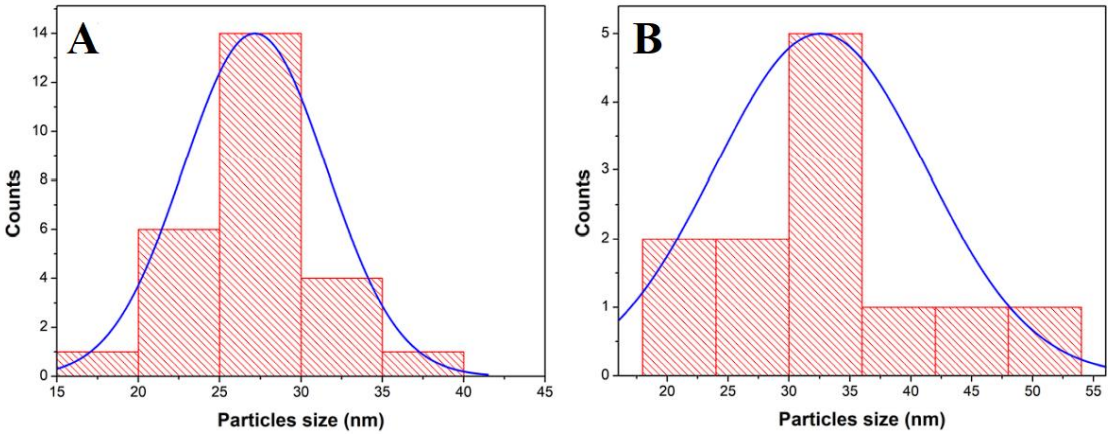

Fig. 4.21 Histogram of particle size distributions of the synthesized AgNPs (A) 1 mM $AgNO_3$ solution (B) 5 mM solution.

The particle size ranges from 15-45 nm for 1 mM $AgNO_3$ and 16-54 nm for 5 mM $AgNO_3$ concentrations. The AgNPs are poly-dispersed. The average particle size is 27 nm and 32.5 nm for 1 mM and 5 mM $AgNO_3$, respectively. This result varied slightly from the average crystallite size calculated from XRD data. This was due to the capping layer of AgNPs originating from the leaf extract. TEM images also revealed that the synthesized AgNPs are less agglomerated, which may be due to the capping agents on the surface of the AgNPs derived from *A. indica* leaf extract.

4.8 TGA and DSC Analysis

TGA and DSC analyses were performed to investigate the thermal behavior and stability of the synthesized AgNPs and AgNPs coated cotton fibers. The samples were heated from 25 to 800 $^{\circ}$C at a rate of 10 $^{\circ}$C /min. This analysis was done in an inert atmosphere of nitrogen gas with a 10 ml/min flow rate. Fig. 4.22 shows the TGA and DSC curves recorded for AgNPs. Synthesized AgNPs showed good thermal stability up to 200 $^{\circ}$C. The first weight loss of about 1% occurred at around 50 to 100 $^{\circ}$C. This decrease in weight may be generally attributed to removing residual water due to evaporation.

Second weight loss was found at around 200 to 500 $^{\circ}$C due to the removal of organic compounds acting as capping and stabilizing agents. The thermal decomposition occurred at that temperature. The weight loss due to that decomposition was followed by a marginal decrease in the mass, which further increased up to 650 $^{\circ}$C [86].

At that stage, AgNPs lose weight abruptly with increasing temperature. Because most of the stabilizing and capping agents were protein molecules, they deformed at relatively low temperatures. No significant weight loss was observed from 500 to 800 °C. TGA curve suggests that most of the organic layer over the surface of AgNPs was dispelled at high temperatures and the overall weight loss was about 20% at 800 °C.

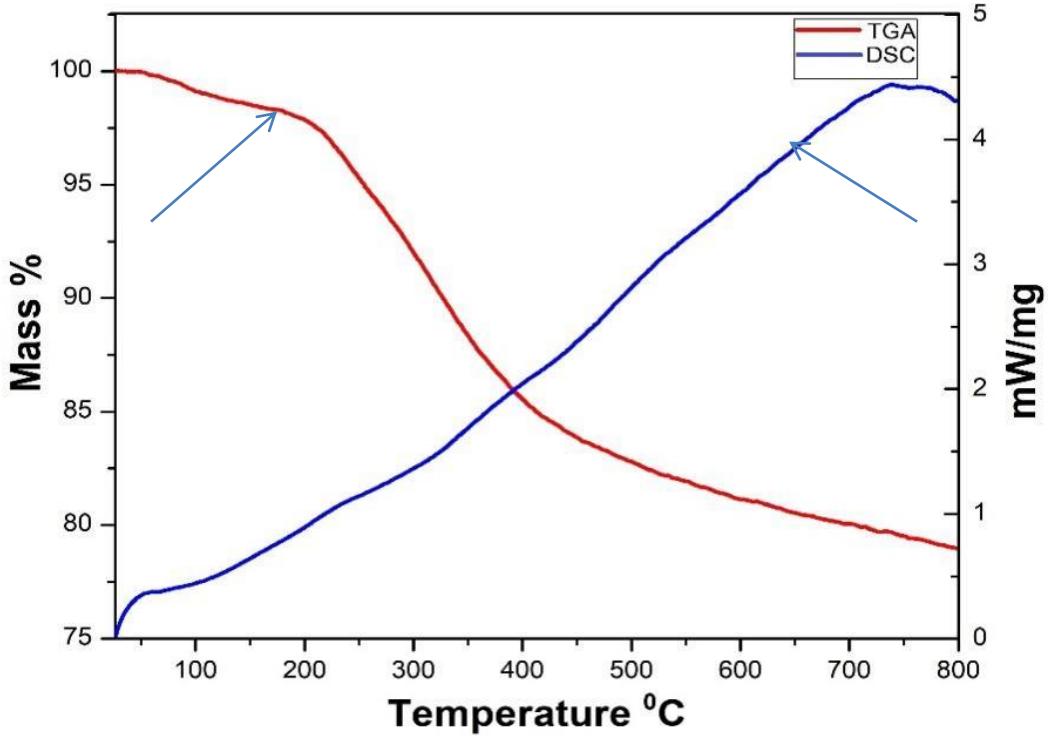

Fig. 4.22 TGA and DSC curve of synthesized AgNPs

Fig. 4.22 illustrated that no endothermic or exothermic peak was observed in the DSC curve of the synthesized AgNPs. It indicates that any crystallographic phase transition did not occur within the temperature range of 25 to 800 °C.

The thermal stability of control cotton fibres and AgNPs incorporated in cotton fibres was tested using TGA. Cotton fibres were thermally stable up to about 200 °C. The mass of the cotton fibres rapidly decreased in the temperature range from 200 to 550 °C. The maximum decomposition of cotton fibres occurred at about 600 °C. Fig. 4.23(A) presents the TGA curve of untreated cotton fibres. On the other hand, AgNPs coated cotton fibres showed good thermal stability up to about 300 °C.

This indicates that the decomposition temperature is higher than the untreated cotton fibres. There was no significant mass loss after 360 °C. The maximum decomposition of AgNPs coated cotton fibres was observed at 800 °C and overall weight loss was about 75% at 800 °C.

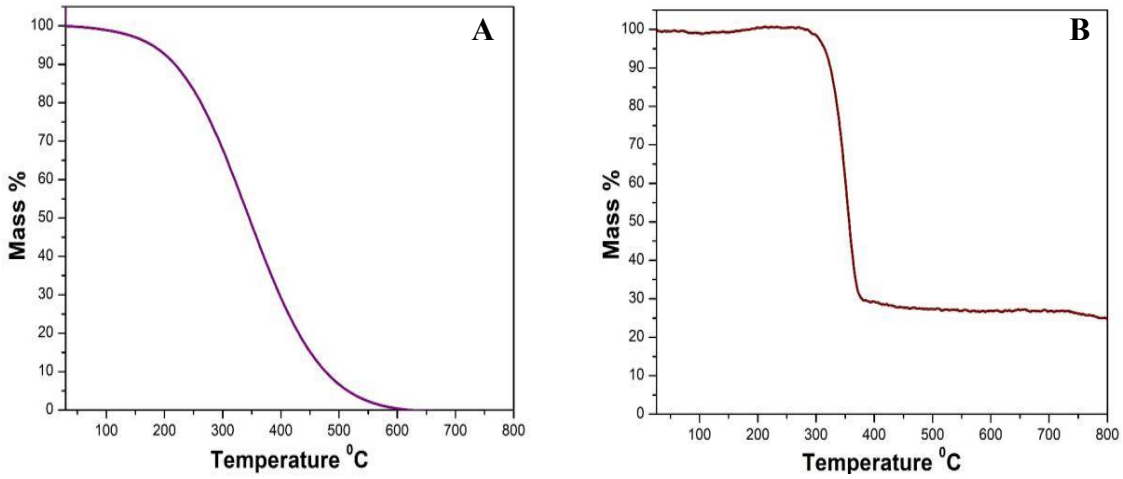

Fig. 4.23 TGA curves of (A) plasma-treated cotton fibres and (B) AgNPs incorporated treated cotton fibres.

This is because the elements present in the leaf extract reduced the Ag+ ions to AgNPs and assisted in binding the synthesized AgNPs onto the surface of the cotton fibres. Therefore, the incorporation of AgNPs into the cotton fibres enhanced their thermal stability. These can be much more applicable to high-temperature conditions. This fabrication methodology is highly successful to exploit AgNPs in textile industries.

4.9 Antibacterial Assay

The antibacterial activity was determined by testing their ability to inhibit the growth of the bacterium. The ability of some bacterial strains to become resistant to antibiotics has a growing interest in finding innovative ways to treat infections. The antibacterial efficacy of AgNPs and AgNPs coated cotton fibres were tested against both Gram-negative (*E. coli*) and Gram-positive (*S. aureus*) bacteria by the Agar well diffusion method. The antibacterial efficiency was assessed by determining the diameter of the clear zone, known as the ZoI. The ZoI was measured using the well diffusion technique, according to Shamaila *et al*. [87]. Antibacterial activity of the synthesized AgNPs against *E. coli* was tested for two different concentrations of $AgNO_3$, 1 mM and 5 mM and they were filled in well 2 and 3, respectively as shown in Fig. 4.24 (A). In the case

of *S. aureus* bacterium, antibacterial activity was tested for three different concentrations of AgNPs (1 mM, 3 mM and 5 mM) as indicated in Fig. 4.24 (B) and they were filled in well 2, 3, and 4, respectively. In both cases, leaf extract was filled in well 1. Each diffusion well on the agar plate was filled with a 25 µL aqueous solution of AgNPs and leaf extract. The biologically synthesized AgNPs showed significant activity compared to leaf extract.

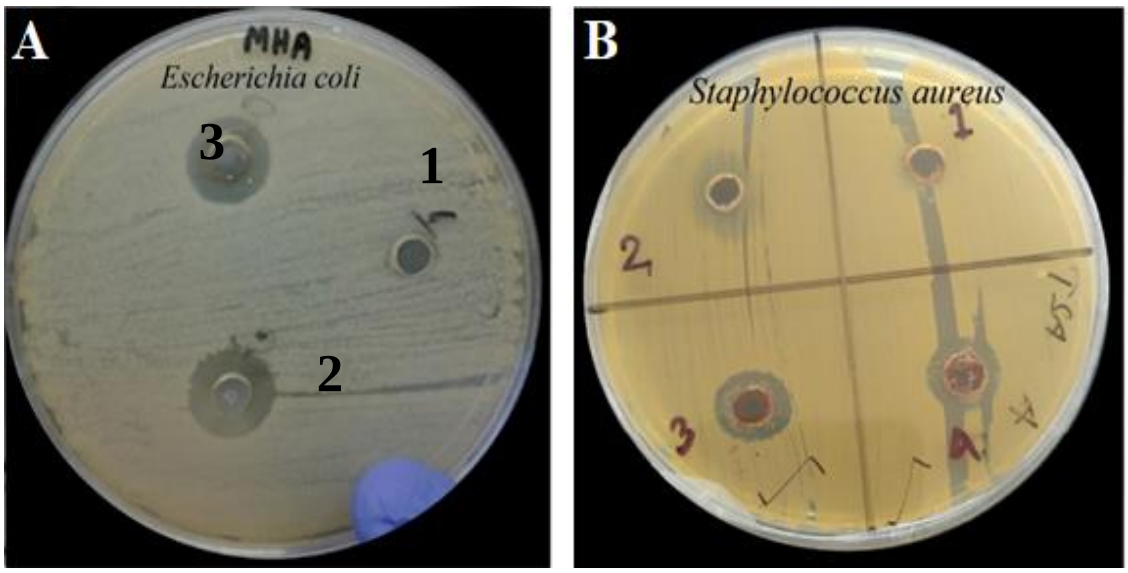

Fig. 4.24 Antibacterial assay against (A) *E.* coli of (1) *A. indica* leaf extract, AgNPs using (2) 1 mM $AgNO_3$, (3) 5 mM $AgNO_3$ solution and (B) *S. aureus.* of (1) *A. indica* leaf extract, AgNPs using (2) 1 mM $AgNO_3$, (3) 3 mM $AgNO_3$ (4) 5 mM $AgNO_3$ solution.

The synthesized AgNPs showed good antibacterial efficacy against both gram-positive and gram-negative bacteria. A clear ZoI was observed around the well on the nutrient agar plates. The ZoI was measured 14 mm against *E. coli* and 12 mm against *S. aureus* bacteria. On the other hand, leaf extract alone did not exhibit any ZoI. According to Roy *et al.* [36] no ZoI was observed for 20 µL AgNPs against *E. coli*, whereas ZoI was 12.5 mm against *S. aureus* for the same amount of AgNPs.

Further, the antibacterial activity of AgNPs coated oxygen plasma-treated cotton fibres was examined. It also exhibited good antibacterial activity against Gram-positive (*S. aureus*) and Gram-negative (*E. coli*) bacteria. The oxygen plasma-treated cotton/AgNPs

fibres were responsible for reducing bacterial growth due to the faster release of silver ions into the medium. The clear ZoI around the cotton fibres suggests the superior antibacterial efficacy of AgNPs coated cotton fibres.

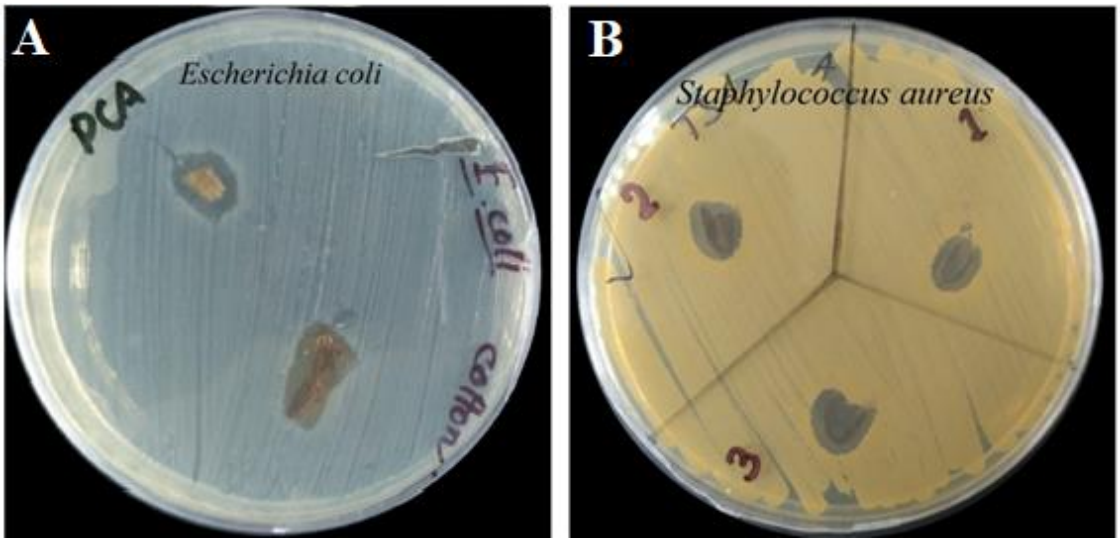

Fig. 4.25 Antibacterial assay for AgNPs coated cotton fibres using 5 mM $AgNO_3$ against (A) *E. coli* and (B) *S. aureus.*

The results of antibacterial activities of synthesized AgNPs and AgNPs cotton fibres against *E. coli* and *S. aureus* bacteria are tabulated below.

Table 4.4 Zone of inhibition against different bacteria

Synthesized AgNPs/ AgNPs incorporated cotton fibres		Zone of inhibition (mm)	
		E. coli	*S. aureus*
Synthesized AgNPs for different concentrations of $AgNO_3$	1 mM	14	ZOI not found
	3 mM	Not tested	12
	5 mM	14	12
AgNPs incorporated cotton fibres		12	10

AgNPs exhibited good antibacterial efficiency due to some of the following mechanisms. Firstly, AgNPs possess a large surface area and for being nano-sized, they can be readily attached to the cell membrane of the bacteria. These AgNPs may release positively charged Ag^+ ions. Due to electrostatic attraction and affinity to sulfur proteins, the released Ag^+ ions can easily get adhered to the negatively charged bacterial cell wall and cytoplasmic membrane of bacteria. This adherence of Ag ions can enhance permeability and initiates the process of disruption of bacterial cell metabolism due to their interaction with macromolecules in the cell such as proteins. The interaction of Ag^+ions with the cell prevent protein synthesis and decrease membrane permeability, which eventually causes cell death [88]. Secondly, Ag^+ ions can deactivate the cellular enzymes, especially the respiratory enzymes which may lead to enzymatic dysfunction [89-92]. Finally, AgNPs may facilitate the release of reactive oxygen species. This ROS can interrupt ATP production and act as a principal agent for the disruption of the cell membrane and DNA modification [92-94]. Because sulfur and phosphorus are the main constituents of DNA, Ag^+ions react with them, resulting interruption of DNA replication and eventually termination of bacterial life. Moreover, Ag ions denature ribosomes in the cytoplasm which may cause the inhibition of protein synthesis [95]. All of the above-mentioned mechanisms ultimately lead to cell death and inhibit bacterial growth.

It was also reported that spherical and hexagonal AgNPs could inhibit the Gram-negative bacteria better than other shaped AgNPs [96]. By comparing the ZoI from Table 4.4, it can be concluded that AgNPs are more effective against Gram-negative bacteria than Gram-positive bacteria. Because, the cell wall of gram-negative bacteria is thinner than that of gram-positive, they show more susceptibility to AgNPs [97]. This difference in antibacterial efficacy against gram-negative and gram-positive bacteria suggests that the uptake of AgNPs plays a vital role in antibacterial activity [98].

The prepared samples showed good efficiency against both Gram-negative and Gram-positive bacteria. So, this technique could be utilized for fabricating antibacterial cotton fibres as well as protective textile materials.

CHAPTER 5

SUMMARY AND CONCLUSIONS

5.1 Summary

In the present study, AgNPs were synthesized at room temperature by the green approach using *A. indica* leaf extract, which acts as an effective reducing and stabilizing agent. Then biosynthesized AgNPs were incorporated into cotton fibres to fabricate antibacterial cotton fibres. The outcome of this investigation is summarized as follows:

- The formation of AgNPs was confirmed using UV-vis spectroscopy analysis. From the UV-vis absorption spectra, SPR was found in the range of 426-443 nm, which ensured the reduction of Ag ions into Ag nanoparticles.
- The X-ray diffraction analysis confirmed the crystalline nature of AgNPs. It exhibits a face-centered cubic crystal structure with preferential orientation along the (111) plane and the average crystallite size was about 20 nm.
- FTIR analysis confirmed the presence of functional groups that performed dual functions of formation and stabilization of AgNPs.
- Zeta potential measurement revealed that the zeta potential of the biosynthesized AgNPs was found to be -23.2 mV. This result suggested that the surface of the AgNPs is negatively charged and moderately stable.
- FESEM and TEM images showed that the biosynthesized AgNPs were spherical and the average particle size ranged from 20 to 30 nm. EDS spectra suggested that the majority of the constituents atom is silver. FESEM images of oxygen plasma-treated cotton fibres showed good adherence to AgNPs on the surface.
- The inclusion of AgNPs into treated cotton fibres improved their thermal stability.
- The biosynthesized AgNPs and AgNPs coated oxygen plasma-treated cotton fibres showed significant antibacterial influence against both gram-positive and gram-negative bacteria.

5.2 Concluding Remarks

AgNPs were synthesized at room temperature using *A. indica* leaf extract by a single-step, eco-friendly, economical green approach and successfully incorporated onto cotton fibres. Synthesized AgNPs and AgNPs coated cotton fibres exhibited prominent antibacterial efficacy against both gram-positive and gram-negative bacteria.

Our prepared samples may therefore be utilized in antibacterial finishing textiles and wound dressing materials.

5.3 Scope for Future Work

Many more plants could be exploited to synthesize nanoparticles from the vast plant diversity. The following studies will be performed for the safe use of AgNPs in the biomedical and other fields:

- The toxicity level of synthesized AgNPs may be identified to make them suitable for human consumption.
- Z-scan measurement may be performed to study the non-linear properties of biosynthesized AgNPs.
- Biosynthesized AgNPs may be incorporated using padding method to compare efficacy with our present study.

References

[01] Rautela, A., Rani, J., and Debnath, M., "Green synthesis of silver nanoparticles from *Tectona grandis* seeds extract: characterization and mechanism of antimicrobial action on different microorganisms," *J. Anal. Sci. Technol.*, vol. 10, pp. 1-10, 2019.

[02] Kaur, A., and Kumar, R., "Enhanced bactericidal efficacy of polymer stabilized silver nanoparticles in conjugation with different classes of antibiotics," *RSC Adv.*, vol. 9, pp. 1095-1105, 2019.

[03] Bar, H., Bhui, D. K., Sahoo, P., De, S. P., Sankar, P., and Misra, A., "Green synthesis of silver nanoparticles using latex of *Jatropha curcas*," *Colloids Surf., A,* vol. 339, pp. 134-139, 2009.

[04] Wang, Y., and Herron, N., "Nanometer-sized semiconductor clusters: materials synthesis, quantum size effects, and photophysical properties," *J. Phys. Chem. A,* vol. 95, pp. 525-532, 1991.

[05] Gaetano, F. D., Ambrosio, L., Raucci, M. G., Marotta, A., and Catauro, M., "Sol–gel processing of drug delivery materials and release kinetics," *J. Mat. Sci. Mat. Med.,* vol. 16, pp. 261-265, 2005.

[06] Krolikowska, A., Kudelski, A., Michota, A., and Bukowska, J., "SERS studies on the structure of thioglycolic acid monolayers on silver and gold," *Surf. Sci.*, vol. 532, pp. 227-232, 2003.

[07] Zhao, G., and Steven Jr, S. E., "Multiple parameters for the comprehensive evaluation of the susceptibility of *Escherichia coli* to the silver ion," *Biometals*, vol. 11, pp. 27-32, 1998.

[08] Akhtar, M. S., Panwar, J., and Yun, Y. S., "Biogenic synthesis of metallic nanoparticles by plant extracts," *ACS Sustain. Chem. Eng.,* vol. 6, pp. 591-602, 2013.

[09] Hayashi, H., and Hakuta, Y., "Hydrothermal synthesis of metal oxide nanoparticles in supercritical water," *Materials,* vol. 3, pp. 3794-3817, 2010.

[10] Lia, J., Wub, Q., and Wuc, J., “Synthesis of nanoparticles via solvo-thermal and hydrothermal methods,” *Handbook of Nanoparticles*, chap. 5, pp. 296-323, 2015.

[11] Grammatikopoulosa, P., Steinhauera, S., Vernieresa, J., Singha, S., and Sowwa, M.,“Nanoparticle design by gas-phase synthesis,” *Adv. Phys. X*, vol. 1, pp. 81-100, 2016.

[12] Zamiri, R., Azmi, B. Z., Ahangar, H. A., Zamiri, G., Husin, M. S., and Wahab, Z. A., “Preparation and characterization of silver nanoparticles in natural polymers using laser ablation,” *Bull. Mater. Sci.,* vol. 35, pp. 727-731, 2012.

[13] Wang, H., Qiao, X., Chen, J., and Ding, S., “Preparation of silver nanoparticles by chemical reduction method,” *Colloids Surf., A,* vol. 256, pp. 111-115, 2005.

[14] Zhang, Z., Shen, W., Xue, J., Liu, Y., Liu, Y., Yan, P., Liu, J., and Tang, J., “Recent advances in synthetic methods and applications of silver nanostructures,” *Nanoscale Res. Lett.,* vol. 13, pp. 1-18, 2018.

[15] Roy, A., Bulut, O., Some, S., Mandal, A. K., and Yilmaz, M. D., “Green synthesis of silver nanoparticles: biomolecule-nanoparticle organization targeting antimicrobial activity,” *RSC Adv.,* vol. 9, pp. 2673-2702, 2019.

[16] Kaler, A., Patel, N., and Banerjee, U. C., “Green synthesis of silver nanoparticles,” *Curr. Res. Info. Pharm. Sci.,* vol. 11, pp. 68-71, 2010.

[17] Mittal, A. K., Bhaumic, J., Kumar, S., and Banerjee, U. C., “Biosynthesis of silver nanoparticles: Elucidation of prospective mechanism and therapeutic potential,” *J. Colloid Interf. Sci.,* vol. 415, pp. 39-47, 2014.

[18] Korbekandi, H., Iravani, S., and Abbasi, S., “Production of nanoparticles using organisms,” *Crit. Res. Biotechnol.,* vol. 29, pp. 279-306, 2009.

[19] Iravani, S., “Green synthesis of metal nanoparticles using plants,” *Green Chem.*, vol. 13, pp. 2638-2650, 2011.

[20] Haefeli, C., Franklin, C., and Hardy, K., “Plasmid determined silver resistance in *Pseudomonas stutzeri* isolated from silver mine*,” J. Bacteriol.* vol. 158, pp. 389-392, 1984.

[21] Moghaddam, A. B., Namvar, F., Moniri, M., Tahir, P. M., Azizi, S., and Mohamad, R.,"Nanoparticles biosynthesis by fungi and yeast: A review of their preparation, properties and medical applications," *Molecules,* vol. 20, pp. 16540-16565, 2009.

[22] Ahmad, A. Mukherjee, P., Senapati, S., Mandal, D., Khan, M. I., Kumar, R., and Sastry, M., "Extracellular biosynthesis of silver nanoparticles using the fungus *Fusarium oxysporum*," *Colloids Surf., B,* vol. 28, pp. 313-318, 2003.

[23] Guilger-Casagrande, M., Germano-Costa, T., Pasquoto- Stigliani, T., Fraceto, L. F., and Lima, R., "Biosynthesis of silver nanoparticles employing *Trichoderma harzianum* with enzymatic stimulation for the control of *Sclerotinia sclerotiorum*," *Sci. Rep.,* vol. 9, pp. 14351-14359, 2019.

[24] Rajput, S., Werezuk, R., Lange, R. M., and McDermott, M. T., "Fungal isolate optimized for biogenesis of silver nanoparticles with enhanced colloidal stability," *Langmuir,* vol. 32, pp. 8688-8697, 2016.

[25] Das, R. K., and Brar, S. K., "Plant mediated green synthesis: modified approaches," *Nanoscale,* vol. 5, pp. 10155-10162, 2013.

[26] Kajani, A. A., Bordbar, A. K., Esfahani, S. H. Z., Khosropour, A. R., and Rajmjou, A., "Green synthesis of anisotropic silver nanoparticles with potent anticancer activity using *Taxus baccata* extract," *RSC Adv.,* vol. 4, pp. 61394-61403, 2014.

[27] Arokiyaraj, S., Arasu, M. V., Vincent, S., Prakash, N. U., Choi, S. H., Oh, Y. K., Choi, K. C., and Kim, K. H., "Rapid green synthesis of silver nanoparticles from *Chrysanthemum indicum* l and its antibacterial and cytotoxic effects: an in vitro study," *Int. J. Nanomed.,* vol. 9, pp. 379-388, 2014.

[28] Pirtarighat, S., Ghammadnia, M., and Baghshahi, S., "Green synthesis of silver nanoparticles using the plant extract of *Salvia spinosa* grown in vitro and their antibacterial activity assessment," *J. Nanostruct. Chem.,* vol. 9, pp. 1-9, 2019.

[29] Rao, B., and Tang, R. C., "Green synthesis of silver nanoparticles with antibacterial activities using aqueous *Eriobotrya japonica* leaf extract," *Adv. Nat. Sci. Nanosci. Nanotechnol.,* vol. 8, pp. 15014-15021, 2017.

[30] Shankar, S. S., Rai, A., Ahmad, A., and Sastry, M., "Rapid synthesis of Au, Ag and bimetallic Au core-Ag shell nanoparticles using Neem (*Azadirachta indica*) leaf broth," *J. Colloid Interf. Sci.* vol. 275, pp. 496-502, 2004.

[31] Shankar, T., Karthiga, P., Swarnalatha, K., and Rajkumar, K., "Green synthesis of silver nanoparticles using *Capsicum frutescence* and its intensified activity against *E. coli*," *Resource Efficient Technol.,* vol. 3, pp. 303-308, 2017.

[32] Ahmad, N., Sharma, S., Alam, K., Singh, V. H., Shamsi, S. F., Mehta, B. R., and Fatma, A., "Rapid synthesis of silver nanoparticles using dried medicinal plant of basil," *Colloids Surf., B,* vol. 81, pp. 81-86, 2020.

[33] Gomathi, M., Rajkumar, P. V., Prakasam, A., and Ravichandran, K., "Green synthesis of silver nanoparticles using *Datura stramonium* leaf extract and assessment of their antibacterial activity," *Resource Efficient Technol.,* vol. 3, pp. 280-284, 2017.

[34] Rajkumar, S. R. S., Sivakumar, N., Selvakumar, G., Selvakumar, T., Sudhakar, C., Ashokkumar, B., and Karthi, S., "Green synthesized silver nanoparticles from *Garcinia imberti* bourd and their impact in root canal pathogens and HepG2 cell lines," *RSC Adv.,* vol. 7, pp. 34548-34555, 2017.

[35] Philip, D., *"*Mangifera indica leaf-assisted biosynthesis of well-dispersed silver nanoparticles,*" Spectrochim. Acta, Part A.,* vol. 78, pp. 327-331, 2011.

[36] Roy, P., Das, B., Mohanty, A., and Mohapatra, S., "Green synthesis of silver nanoparticles using *Azadirachta indica* leaf extract and its antibacterial study," *Appl. Nanosci.,* vol. 7, pp. 843-850, 2017.

[37] Banerjee, P., Satapathy, M., Mukhopahayay, A., and Das, P., "Leaf extract mediated green synthesis of silver nanoparticles from widely available Indian plants: synthesis, characterization, antimicrobial property and toxicity analysis," *Bioresour. Bioprocess.,* vol. 1, pp. 1-10, 2014.

[38] Lewis, K., and Klibanov, A. M., “Surpassing nature: rational design of sterile-surface materials,” *TRENDS Biotechnol.,* vol. 23, pp. 343-348, 2005.

[39] Thomas, V., Bajpai, S. K., Mohan, Y. M., and Sreedhar, B., “A versatile strategy to fabricate hydrogel-silver nanocomposites and investigation of their antimicrobial activity,” *J. Colloid Interf. Sci.,* vol. 315 pp. 389–395, 2007.

[40] Duran, N., Marcato, P. D., De Souza, G. I. H., Alves, O. L., and Esposito, E., “Antibacterial effect of silver nanoparticles produced by fungal process on textile fabrics and their effluent treatment,” *J. Biomed. Nanotechnol.,* vol. 3, pp. 203–208, 2007.

[41] Czajka, R., “Development of medical textiles,” *Fib. Text. East. Eur.,* vol. 13, pp. 13–15, 2005.

[42] Gao, Y., and Cranston, R., “Recent advances in antimicrobial treatments of textiles,” *Text. Res. J.* vol. 78, pp. 60–72, 2008.

[43] Gorenˇsek, M., and Recelj, P., “Nanosilver functionalized cotton fabric,” *Text. Res. J.,* vol. 77, pp. 138–141, 2007.

[44] Wu, Y., Yang, Y. Zhang, Z., Wang, Z., Zhao, Y., and Sun, L., “Fabrication of cotton fabrics with durable antibacterial activities finishing by Ag nanoparticles,” *Tex. Res. J.*, vol. 89, pp. 867-880, 2018.

[45] El-Rafie, M. H., Shaheen, T. I., Mohamed, A. A., and Hebeish, A., “Bio-synthesis and applications of silver nanoparticles onto cotton fabrics”, *Carbohydr. Polym.,* vol. 90, pp. 915-920, 2012.

[46] Ravindra, S., Mohan, Y. M., Reddy, N. N., and Raju, K. M., “Fabrication of antibacterial cotton fibres loaded with silver nanoparticles via “Green Approach”, *Colloids Surf., A,* vol. 367, pp. 31-40, 2010.

[47] Zafar, M. T., Maiti, S. N., and Ghosh, A. K., “Effect of surface treatment of jute fibers on the interfacial adhesion in poly(lactic acid)/jute fiber biocomposites,” *Fibers Polym.,* vol. 17, pp. 266-274, 2016.

[48] Nowack, B., Krug, H. F., and Height, M., “120 years of nanosilver history: Implication for policy makers,” *Environ. Sci. Technol.*, vol. 45, pp. 1177-1183, 2011.

[49] Henglein, A., “Small-particle research: physicochemical properties of extremely small colloidal metal and semiconductor particles,” *Chem. Rev.*, vol. 89, pp. 1861-1873, 1989.

[50] Mulvaney, P., “Surface plasmon spectroscopy of nanosized metal particles,” *Langmuir*, vol. 12, pp. 788-800, 1996.

[51] Balamurugan, M., Saravanan, S., and Soga, T., “Coating of green-synthesized silver nanoparticles on cotton fabric,” *J. Coat. Technol. Res.*, vol. 14, pp. 735-745, 2017.

[52] Karahan, H. A., and Özgoğan, E., “Improvements of surface functionality of cotton fibres by atmospheric plasma treatment,*” Fibres Polym.*, vol. 9, pp. 21-26, 2008.

[53] Lai, C. Y., Sapuan, S. M., Ahmad, M., Yahya, N., and Dahlan, K. Z. H. M., “Mechanical and electrical properties of coconut coir fiber-reinforced polypropylene composites,” *Polym. Plast. Technol. Eng.*, vol. 44, pp. 619–632, 2005.

[54] Sun, D., and Stylios, G. K., “Effect of low temperature plasma treatment on the scouring and dyeing of natural fabrics,” *Text. Res. J.*, vol. 74, pp. 751-756, 2004.

[55] Karahan, H.A., Ozdogan, E., Demir, A., Ayhan, H., and Seventekin, N., “Effects of atmospheric plasma treatment on the dyeability of cotton fabrics by acid dyes,” *Color. Technol*., vol. 124, pp. 106-110, 2008.

[56] Tsafack, M. J., and Levalois-Grützmacher, J., “Towards multifunctional surfaces using the plasma-induced graft-polymerization (PIGP) process: Flame and waterproof cotton textiles,” *Surf. Coat. Technol*., vol. 201, pp. 5789-5795, 2007.

[57] Ražić, S. E., Čunko, R., Bukošek, V., and Matica, B., “Antimicrobial modification of cellulose fabrics using low-pressure plasma and silver compounds,” *Tekstil.*, vol. 60, pp. 427-440, 2011.

[58] Ražić, S. E., Čunko, R., Bautista, L., and Bukošek, V., "Plasma effect on the chemical structure of cellulose fabric for modification of some functional properties," *Procedia Eng.*, vol. 200, pp. 333-340, 2017.

[59] Jajbec, K., Sala, M., Mozetic, M., Vesel, A., and Gorjanc, M., "Functionalization of cellulose fibres with oxygen plasma and ZnO nanoparticles for achieving UV protective properties," *J. Nanomater.,* vol. 2015, pp. 9, 2015.

[60] Michael, B., Peter, L., and Dieter, N., "Analytical application of Fourier transform infrared (FT-IR) spectroscopy in microbiology and prion research", *Vet. Microbiol.,* vol. 123, pp. 305-319, 2001.

[61] Cullity, B. D. (1959) *Elements of X-ray Diffraction*, Addison-Wesley Publishing Company. Inc, U. S. A.

[62] David, H., "Crystal structure determination", *J. pure Appl. Phys.,* vol. 6, pp. 187-282, 1959.

[63] Josi, P., Esteban, B., and Teresa, J. A., "Antimicrobial activity of seven root canal sealers results of agar diffusion and agar dilution tests," *Endodontics,* vol. 74, pp. 216-220, 1992.

[64] Nassar, M. S. M., Hazzah, W. A., and Bakr, W. M. K., "Evaluation of antibiotic susceptibility test results: how guilty a laboratory could be?," *J. Egyptian Public Health Association,* vol. 94, pp. 1-5, 2019.

[65] Ravichandran, V., Vasanthi, S., Shalini, S., Shah, S. A. A., and Harish, R., "Green synthesis of silver nanoparticles using Atrocarpus altilis leaf extract and the study of their antimicrobial and antioxidant activity," *Mater. Lett.*, vol. 180, pp. 264-267, 2016.

[66] Verma, A., and Mehta, M. S., "Controllable synthesis of silver nanoparticles using neem leaves and their antimicrobial activity," *J. Rad. Res. Appl. Sci.,* vol. 9, pp. 109-115, 2016.

[67] Poopathi, S., Brito, L. J. D., Praba, V. L., Mani, C., and Praveen, M., "Synthesis of silver nanoparticles from *Azadirachta indica*-a most effective method for mosquito control," *Environ. Sci. Pollut. Res.*, vol. 22, pp. 2956-2963, 2014.

[68] Anandan, M., Poorani, G., Boomi, P., Varunkumar, K., Anand, K., Chuturgoon, A. A., Saravanan, M., and Prabu, H.G., "Green synthesis of anisotropic silver nanoparticles from the aqueous leaf extract of *Dodonaea viscosa* with their antibacterial and anticancer activities," *Process Biochem.*, vol. 80, pp. 80-88, 2019.

[69] Kelly, L., Coronado, E., Zhao, L. L., and Schatz, G. C., "The optical properties of metal nanoparticles: the influence of size, shape and dielectric environment," *J. Phy. Chem. B.*, vol. 107, pp. 668-677, 2003.

[70] Sarkar, S., and Kotteeswaran, V., "Green synthesis of silver nanoparticles from aqueous leaf extract of Pomegranate (*Punica granatum*) and their anticancer activity on human cervical cancer cells", *Adv. Nat. Sci.: Nanosci. Nanotechnol.* vol. 9, pp. 025014-025023, 2018.

[71] Elamawi, R. M., Al-Harbi, R. E., and Hendi, A. A., "Biosyntheis and characterization of silver using *Trichoderma longibrachiatum* and effect on phytopathogenic fungi," *Egyptian J. Bio. Pest Control*, vol. 28, no. 28, 2018.

[72] Yeshchenko, O. A., Dmitruk, I. M., Alexeenko, A. A., Kotko, A. V., Verdal, J., and Pinchuk, A. O., "Size and Temperature Effects on the Surface Plasmon Resonance in Silver Nanoparticles," *Plasmonics*, vol. 7, pp. 685-694, 2012.

[73] Luo, Y., Shen, S., Luo, J., Wang, X., and Sun, R., "Green synthesis of silver nanoparticle in xylan solution via Tollens reaction and its detection for Hg^{2+}," *Nanoscale*, vol. 7, pp. 690-700, 2015.

[74] Goudarzi, M., Mir, N., Kamazani, M. M., Bagheri, S., and Niasari, M. S., "Biosynthesis and characterization of silver nanoparticles prepared from two novel natural precursor by facile thermal decomposition methods," *Sci. Rep.*, vol. 6, pp. 32539-32551, 2016.

[75] Melendrez, M. F., Gardenas, G., and Arbiol, J., “Synthesis and characterization of gallium colloidal nanoparticles”, *J. Colloid Interf. Sci.*, vol. 346, pp. 279-287, 2010.

[76] Singh, H., Du, J., Singh, P., and Yi, T. H., “Role of green silver nanoparticles synthesized from *Symphytum officinale* leaf extract in protection against UVB-induced photoaging”, *J. Nanostruct. Chem.*, vol. 8, pp. 359-368, 2018.

[77] Sathishkumar, M., Sneha, K., Won, S. W., Cho, C-W., Kim S., and Yun, Y-S., “Cinnamon zeylanicum bark extract and powder mediated green synthesis of nano-crystalline silver particles and its bactericidal activity”, *Colloids Surf., B*, vol. 73, pp. 332-339, 2009.

[78] Suresh, A. K., Doktycz, M. J., Wang, W., Moon, J. W., Gu, B., Meyer, H. M., Hensley, D. K., Allison, D. P., Phelps, T. J., and Pelletier, D. A., “Monodispersed biocompatible silver sulfide nanoparticles: facile extracellular biosynthesis using the γ-proteobacterium *Shewanella oneidensis*”, *Acta Biomater*., vol. 7, pp. 4253–4258, 2011.

[79] Meng, Y., “A Sustainable Approach to Fabricating Ag Nanoparticles/PVA Hybrid Nanofiber and Its Catalytic Activity,” *Nanomater.*, vol. 5, pp. 1124-1135, 2015.

[80] Anandalakshmi, K., Venugobal, J., and Ramasamy, V., “Characterization of silver nanoparticles by green synthesis method using Pedalium murex leaf extract and their antibacterial activity,” *Appl. Nanosci.*, vol. 6, pp. 399-408, 2016.

[81] Heidarpour, F., Ghani, W. A. W. Ab. Karim., Ahmadun, F. R. Bin., Sobri, S., Zargar, M., and Mozafari, M. R., “Nano silver-coated polypropylene water filter: I. Manufacture by electron beam gun using a modified balzers 760 machine,” *Digest J. Nanomater. & Biostruct.*, vol. 5, pp. 787-796, 2010.

[82] Hui, Y., Yan-yu, R., Tao, W., and Chuang, W., “Preparation and antibacterial activities of Ag/Ag+/Ag3+ nanoparticle composites made by pomegranate (*Punica granatum*) rind extract,” *Results Phys.*, vol. 6, pp. 299-304, 2016.

[83] Kumar, V., and Yadav, S. K., "Plant-mediated synthesis of silver and gold nanoparticles and their applications," *J. Chem. Technol. Biotechnol.,* vol. 84, pp. 151-157, 2009.

[84] Juttula, H. J., Tormanen, M., and Makynen, A. J., "Predicting scattering properties of fiber suspensions using Mie theory and probabilistic cross-sectional diameter of fibers," *Opt. Rev.,* vol. 27, pp. 225-232, 2020.

[85] Wang, M., Li, H., Li, Y., Mo, F., Li, Z., Chai, R., and Wang, H., "Dispersibility and size control of silver nanoparticles with anti-algal potential based on coupling effects of polyvinylpyrrolidone and sodium tripolyphosphate," *Nanomater.,* vol. 10, pp. 1042-1056, 2020.

[86] Kota, S., Dumpala, P., Anantha, R. K., Verma, M. K., and Kandepu, S., "Evaluation of therapeutic potential of the silver/silver chloride nanoparticles synthesized with the aqueous leaf extract of Rumex acetosa," *Sci. Rep.,* vol. 7, pp. 11853-11863, 2019.

[87] Shamaila, S., Zafar, N., Riaz, S., Sharif, R., Nazir, J., and Naseem, S., "Gold nanoparticles: An efficient antimicrobial agent against enteric bacterial human pathogen," *Nanomater*., vol. 6, pp. 71-80, 2016.

[88] Su, H. L., Chou, C. C., Hung, D. J., Lin, SH., Pao, I. C., Lin, J. H., Huang, F. L., Dong, R. X., and Lin, J. J., "The disruption of bacterial membrane integrity through ROS generation induced by nanohybrids of silver and clay," *Biomater*., vol. 30, pp. 5979–5987, 2009.

[89] Rajoriya, P., "Green synthesis of silver nanoparticles, their characterization and antimicrobial potential", *PhD. Thesis*, Department of Molecular & Cellular Engineering, Sam Higginbottom University of Agriculture, Technology & Sciences, 2017.

[90] Gordon, O., Slenters, V. T., Brunetto P. S., Villaruz, A. E., Sturdevant, D. E., Otto, M., Landmann, R., and Fromm, K. M., "Silver coordination polymers for the prevention of implant infection: thiol interaction, impact on respiratory chain enzymes, and hydroxyl radical induction," *Antimicrob. Agents Chemother*., vol. 54, pp. 4208–4218, 2010.

[91] Hossain, Z., and Huq, F., "Studies on the interaction between $Ag^{(+)}$ and DNA," *J. Inorg. Biochem.*, vol. 91, pp. 398–404, 2002.

[92] Pal, S., Tak, Y. K., and Song, J. M., "Does the antibacterial activity of silver nanoparticles depend on the shape of the nanoparticle? A study of the Gram-negative bacterium *Escherichia coli*," *Appl. Environ. Microbiol.* vol. 73, pp. 1712–1720, 2007.

[93] Khorrami, S., Zarrabi, A., Khaleghi, M., Danaei, M., and Mozafari, M., "Selective cytotoxicity of green synthesized silver nanoparticles against the MCF-7 tumor cell line and their enhanced antioxidant and antimicrobial properties," *Int. J. Nanomed.*, vol.13, pp. 8013–8024, 2018.

[94] Ramkumar, V. S., Pugazhendhi, A., and Gopalakrishnan, K., "Biofabrication and characterization of silver nanoparticles using aqueous extract of seaweed Enteromorpha compressa and its biomedical properties," *Biotechnol. Rep.*, vol. 14, pp. 1–7, 2017.

[95] Durán, N., Nakazato, G., and Seabra, A., "Antimicrobial activity of biogenic silver nanoparticles, and silver chloride nanoparticles: an overview and comments," *Appl. Microbiol. Biotechnol.*, vol. 100, pp. 6555–6570, 2016.

[96] Pal, S., Tak, Y. K., and Song, J. M., "Does the antibacterial activity of silver nanoparticles depend on the shape of the nanoparticle? A study of the Gram-negative bacterium *Escherichia coli*," *Appl. Environ. Microbiol.* vol. 73, pp. 1712–1720, 2007.

[97] Meikle, T., Dyett, B. P., Strachan, J. B., White, J., Drummond, C. J., Conn, C. E., "Preparation, characterization, and antimicrobial activity of cubosome encapsulated metal nanocrystals," *ACS Appl. Mater. Interf.*, vol. 12, pp. 6944–6954, 2020

[98] Noronha, V. T., Paula, A. J., and Durán, G., "Silver nanoparticles in dentistry," *Dent. Mater.*, vol. 33, pp. 1110–1126, 2017.